UNIVERSITY OF MINNESOTA
ST. ANTHONY FALLS LABORATORY
Engineering, Environmental and Geophysical Fluid Dynamics

Project Report No. 414

Gas Transfer Measurements at Hydraulic Structures on the Ohio River

by

Suresh L. Hettiarachchi, John S. Gulliver, David E Hibbs
St. Anthony Falls Laboratory, Department of Civil Engineering, University of Minnesota
Minneapolis, Minnesota.

John Howe, Summit Envirosolutions, Minneapolis, Minnesota
Kimberly F Miller, U.S. Geological Survey, Charleston, West Virginia
George P. Kincaid, U.S. Army Corps of Engineers, Hungtington, West Virginia

Prepared for

U. S. ARMY CORPS OF ENGINEERS
Hungtington District
Huntington, West Virginia

Contract No. DA/DACW69-96-P-1410

June1998
Minneapolis, Minnesota

Prepared for: Metropolitan Council
Last Revised: 6/30/98
Disk Locators: Ohio\PR414txt.doc; PR414COV.doc
(Zip Disk #10/Figures)

ABSTRACT

Gas transfer at hydraulic structures has been a topic of interest for many years. Navigation dams on rivers can add a large amount of atmospheric gases to the water due to the high velocities and the turbulence generated as the water passes through these structures. The increase in air-water gas transfer is due to air entrainment and the formation of bubbles in the flow. Hence, gas transfer at hydraulic structures plays an important role in the water quality of a river-reservoir system.

Measurement of air-water gas transfer at hydraulic structures is a complicated process. Oxygen has, historically, been the measured gas, but concentration levels close to saturation and significant vertical stratification in oxygen concentration in the upstream pool often hinder accurate transfer measurements. The U.S. Army Corps of Engineers, The U.S. Geological Survey, and the University of Minnesota have been involved in this project to measure gas transfer at hydraulic structures in the Ohio River basin, using in-situ methane as a tracer in addition to measuring dissolved oxygen. The use of the two volatile chemicals increases the possibility of worthwhile field measurements. This project is conducted in order to evaluate gas transfer characteristics at various hydraulic structures on the Ohio River so that spills through the gates can be optimized. The hydropower producers on the Ohio River may also benefit from this information, as wastage of water from the reservoir to meet water quality requirements will be minimized.

The results show that gas transfer increases significantly when a hydraulic jump forms in the stilling basin at gated sill structures, which is the type most commonly seen on the Ohio River. It is also clear that gas transfer at hydraulic structures is significantly affected by the structural characteristics and the hydraulic action at each site.

ACKNOWLEDGMENTS

The Summit Envirosolutions individuals who participated in the measurements were Chris Ryndell, and Mike Hayes. The USGS employees who aided the data collection were Carl Faulkenburg, John T Atrkins, Melvin Mathis, and Eddie Pucket. Also, Buddy Hill, Rich Meyer and Pat Nector of the USACE provided additional support.

TABLE OF CONTENTS

LIST OF FIGURES

LIST OF TABLES

LIST OF VARIABLES

C	Concentration
C_s	Saturation Concentration
K_L	Liquid mass transfer coefficient
C_u	Concentration upstream of the structure
C_d	Concentration downstream of the structure
E	Transfer efficiency
E_i	Indexed transfer efficiency
f_i	Indexing factor
D	Diffusivity of compound in water
D_i	Diffusivity of indexing compound in water
P_b	Mean pressure on the bubbles in at depth
P_{atm}	Atmospheric pressure
d_{eff}	Effective depth
C_{se}	effective saturation concentration
A	Area of bubble swarm used to calculate the first moment of the bubble swarm about the tailwater elevation
Cent	Centroid of the bubble swarm calculated by the first moment of the bubbles swarm about the tailwater elevation
y_1	Gate opening
y_b	Height of the endsill
y_3	The depth of water downstream of the stilling basin
TWD	Tailwater depth in the stilling basin
d	height at the sill
β	Fixed parameter
$X_{1/2}$	Effective length
q	Specific flow rate
v_r	Rise velocity of bubbles in a turbulent flow
RF	Gas chromatograph response factor

V_{inj}	Sample volume injected in to the gas chromatograph
V_{HS}	Headspace volume in the vial
H_{lc}	Henry's law constant
U_m	Measurement uncertainty
U_p	Precision uncertainty
U_B	Bias uncertainty
U_{HFC}	Uncertainty in headspace correction factor
U_{EH}	Uncertainty in Henry's law constant
U_{cal}	Calibration uncertainty
t_{n-1}	Students t score
σ	Standard deviation of the methane injections
σ_x	Standard deviation of the oxygen measurement about the depth averaged mean
U_m	Uncertainty in mean concentration
U.S.	Sampling uncertainty
U_{mu}	Uncertainty in measured concentration upstream
U_{md}	Uncertainty in measured concentration downstream
U_E	Uncertainty in calculated transfer efficiency
U_X	Uncertainty in measured oxygen percent saturation
U_{xd}	Uncertainty in predicted oxygen concentration downstream
U_{Eo}	Uncertainty in indexed transfer efficiency

INTRODUCTION

Dissolved oxygen (DO) is an important water quality parameter in rivers and reservoirs. Many of the biological processes that maintain good water quality consumes DO in the water. Therefore the lack of DO will result in poor water quality. Aeration, which is the process by which oxygen is absorbed by water from the atmosphere, is important to maintain DO at a suitable level. Water quality and DO levels are concerns in the Ohio River basin as the Ohio River valley is one the most developed basins in North America with a high population density and a significant level of industrialization and pollution (Kissel 1991). In addition, many of the upstream pools at the Lock and Dam structures on the Ohio River are widely used for recreational fishing.

Normal atmospheric aeration (reaeration) is a very slow process in a river-reservoir system. Aeration must occur over many miles before a significant amount of air-water oxygen transfer takes place. In contrast, significant amounts of aeration can occur as water flows past hydraulic structures such as locks and dams. The main reason for this increase is that air gets entrained in the flow as illustrated in figure 1. The flow also experiences very high velocities which generate high turbulence levels increasing the flux rate and breaking up the entrained air into small bubbles. The formation of smaller bubbles increases the interfacial surface area available for gas transfer, hence the significant increase in gas transfer. This increase in surface area due to bubbles has been estimated to be roughly 500 times the free surface area exposed to the atmosphere at one hydraulic structure (Gulliver et al 1990).

The Ohio River has a total of over 50 lock and dam structures constructed by the U.S. Army Corps of Engineers for navigation and flood control (Kissel 1991). These structures changed the Ohio River into a series of pools instead of a free flowing river , which also furnish a significant potential for hydropower generation. The effect of water flowing through these hydraulic structures on reaeration plays a major role in maintaining DO levels in the Ohio river. For example, a large spill of water through the gates might be required to reaerate the water and achieve the required DO concentrations (Railsback 1991). Balancing between the need for hydropower generation, navigation, and maintaining favorable water quality levels is difficult, especially during low flow periods. Therefore, in order to develop efficient spill patterns and to utilize the water resource in the most beneficial manner, it is important to quantify the Reaeration capabilities and understand the reaeration characteristics of these hydraulic structures on the Ohio River

There has been interest in the reaeration of hydraulic structures on the Ohio River for many years. The first reported measurements are those of Holler (1969). An examination of these measurements point out the difficulty in obtaining quality measurements of gas transfer through the measurement of DO at a large hydraulic structure(Gulliver and Wilhelms 1992). First, lateral variations in the concentration in

the reservoir and tailwater, when present, can bias the result unless large number of samples are collected over space. Second, vertical stratification of DO, which occurs often in these reservoirs, can result in significant measurement uncertainties.

Figure 1. Picture of air entrainment in a hydraulic jump (Hoyt and Selin 1989)

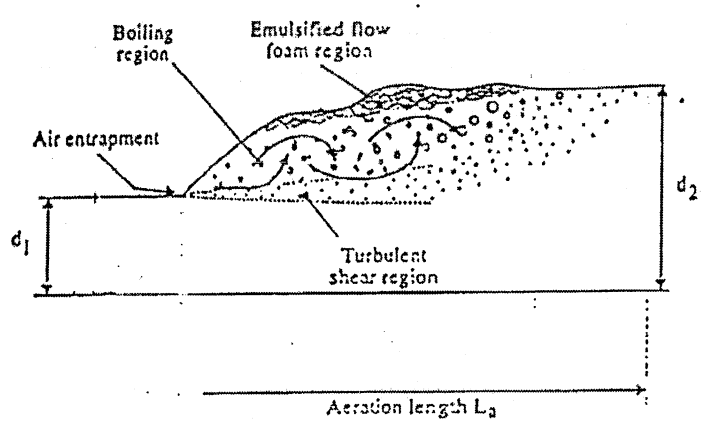

Figure 2. Illustration of air entrainment in a hydraulic jump

The U.S. Army Corps of Engineers, The U.S. Geological Survey and the Hydropower producers are working to determine the oxygen transfer characteristics of the hydraulic structures on the Ohio River and other rivers in the basin. As a means of quantifying the ability of lock and dam structures in the Ohio River system to add oxygen to passing flows, the reaeration potential of nine hydraulic structures were evaluated using *in situ* methane as a surrogate tracer for DO as well as DO measurements. The following discusses the measurements carried out, the results of these measurements, and the analysis of the reaeration characteristics at the hydraulic structures studied on the Ohio River. The results are presented as transfer efficiencies at each of the structures with associated uncertainties. Detailed results of the measurements and structural data significant to gas transfer at each site are given in the appendices. A qualitative explanation of the gas transfer process at each of these structures is also presented.

GAS TRANSFER AT HYDRAULIC STRUCTURES

Making the assumption that the gas is volatile ($K_L >> Hk_g$) and that the gas mole fraction inside the entrained bubbles does not change significantly(Gulliver et al 1997), the concentration gradient in a control volume moving over the structure is given by:

$$\frac{dC}{dt} = K_L a(C_s - C) \tag{1}$$

where a is the specific surface area, K_L is the liquid film coefficient, and dC/dt is the rate of change of the concentration. The second assumption is the more strict for gas transfer at hydraulic structures. Gulliver, at al (1997) estimated that this assumption would be valid for a compound with a dimensionless Henry's Law partitioning constant of roughly 15 and above at a spillway plunge pool.

An integration and rearrangement of equation 1 over the residence time of a water element from upstream to downstream results in a transfer efficiency, (Thompson and Gulliver, 1997):

$$E = \frac{C_d - C_u}{C_s - C_u} = 1 - \exp(-\int_{td}^{tu} K_L a dt) \tag{2}$$

where C_u is the upstream concentration , C_d is the downstream concentration, and t is the residence time of the bubbles. Although unnecessary, it is often informative to convert equation 2 into the equation for transfer efficiency originally developed by Gameson (1957) by assuming that $K_L a$ is a constant over the hydraulic structure:

$$E = \frac{C_d - C_u}{C_s - C_u} = 1 - e^{-K_L at} \tag{3}$$

where E is the transfer efficiency such that E = 1 means that 100% of the initial deficit in gas concentration (C_s - C) in the upstream water was transferred as the water passes the structure. E = 0 means that no gas transfer occurred. For gases not significantly present in the atmosphere such as methane, equation 3 can be written in the form:

$$E = \frac{C_u - C_d}{C_u} = 1 - e^{K_L at} \tag{4}$$

OXYGEN TRANSFER EFFICIENCY FROM METHANE ANALYSIS

Use of Methane as a Tracer

Gas transfer at hydraulic structures has been studied over a number of years. Gulliver and Wilhelms (1992) discussed the difficulty of obtaining quality measurements of gas transfer at large hydraulic structures using DO. The main reason is that DO is quite often significantly stratified vertically in the upstream reservoir. Opening a gate to spill will pass water from all depths, although in uncertain proportions. Thus the vertical stratification of DO can greatly increase the uncertainty of the upstream DO measurement. Also, DO has a significant equilibrium value and DO concentrations in the upstream pool are quite often close to this equilibrium (saturation). When the upstream DO concentration is close to saturation, the amount of gas transfer that takes place across the structure and the change in concentration are small. This will increase the uncertainty in the gas transfer calculations.

The use of *in situ* methane as a tracer solves quite a few of the above mentioned problems. Field measurements (Gulliver et al., 1997) indicate that methane typically is not strongly stratified in a shallow reservoir. Also, the amount of methane in the atmosphere is negligible when compared to measured concentrations. Finally, methane transfer measurements can be indexed to oxygen transfer efficiency as discussed below. Therefore, methane can be used as a viable tracer for gas transfer at large hydraulic structures.

Indexing Transfer Efficiency

The measured transfer efficiency of methane can be directly converted to other compounds using the relationship developed by Gulliver et al. (1990) for self aerated flow, where the indexed transfer efficiency is related to the measured transfer efficiency such as:

$$E_i = 1 - (1 - E)^{1/f_i} \tag{5}$$

where E_i is the indexed transfer efficiency, E is the measured transfer efficiency, and

$$f_i = \frac{K_L a}{K_L a_i} \tag{6}$$

where the subscript indicates the indexing compound (in this case oxygen). When both the measurement and the computed indexed transfer efficiency are at the same temperature, equation 6 can be written in the form:

$$f_i = \left(\frac{D}{D_i}\right)^{1/2} \quad (7)$$

where D is the molecular diffusivity of the measured compound and D_i is the molecular diffusivity of the indexed compound. For methane and oxygen, $f_i \cong .88$ when the water temperature is similar.

Effects of Plunge Depth of the Bubbles

To obtain the true transfer efficiency of atmospheric gases using equation (3), the effect of the plunge depth of the bubbles must be considered. When the bubbles travel deep into the tailwater, the added hydrostatic pressure increases the saturation concentration of the gases in the bubble. The hydrostatic and the dynamic pressure acting on the bubble is accounted for by using an effective bubble depth, (Gulliver et al., 1997). Using the effective depth, the weighted mean bubble pressure in a plunge pool is given by:

$$P_b = P_{atm} + \gamma d_{eff} \quad (8)$$

where P_b is the mean pressure in the bubbles weighted by its impact upon gas transfer, P_{atm} is the atmospheric pressure, and γd_{eff} is the additional hydrostatic pressure.

An effective saturation concentration (C_{se}) which corresponds to the increase in saturation concentration due to the added pressure on the bubble may be defined. The effective saturation concentration is related to the effective depth by (Gulliver et al., 1997):

$$\frac{C_{se}}{C_s} = \frac{\gamma d_{eff}}{P_{atm}} + 1 \quad (9)$$

where C_{se} is the effective saturation concentration and C_s is the local saturation concentration of the gas at atmospheric pressure.

The results of the above relationships are contingent upon the accurate determination of the effective depth. The process of estimating d_{eff} for the structures in the study is discussed below.

Effective Depth at Gated Sills

Determining the plunge depth accurately is not straight-forward at the gated sill structures that predominate on the Ohio River. The flow patterns along the drop at the sill and the mechanism for air entrainment are quite different from other hydraulic structures. Hibbs and Gulliver (1995) developed a formula to predict the effective bubble depth in a stilling basin with a plunge pool flow. As the flow patterns at gated sills are different from those in spillway plunge pools, the bubbles do not plunge to the maximum depth of the stilling basin. Figure 1 illustrates the point where the bubbles entrained by a hydraulic jump follow a pattern close to a surface jet. Hibbs and Gulliver (1995) and

Roesner and Norton (1971) used the centroid of the expected bubble swarm in the stilling basin for plunging flows with good results at large gate openings. Using pictures of air entrainment and bubble distributions in figure 1 and the structural characteristics, speed and angle of the discharge jet, a bubble swarm pattern was assumed such as presented in figure 3. Half the river depth was used as the effective depth downstream of the stilling basin as the bubbles will be described as uniformly distributed vertically due to the added mixing caused by the turbulence created when the jet interacts with the baffle blocks and the endsill.

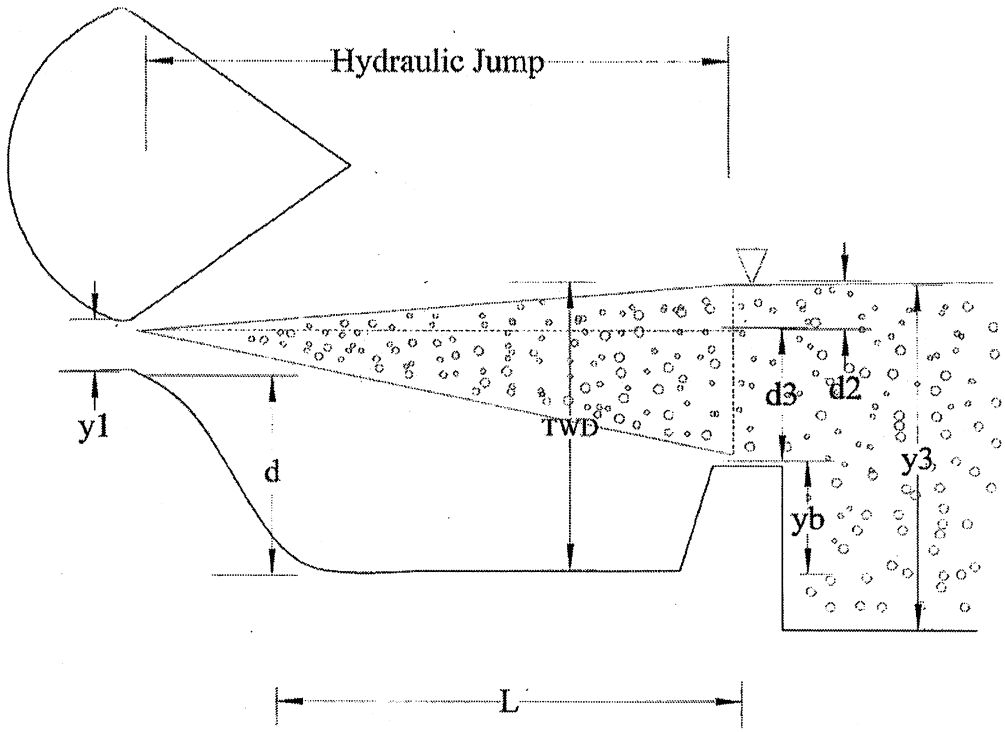

Figure 3. Bubble swarm downstream at a gated sill structure

The centroid of the bubble swarm in the stilling basin is given by the first moment of the bubble swarm about the tailwater elevation:

$$Cent = \frac{A_1 Cent_1 + A_2 Cent_2}{A_1 + A_2} \tag{10}$$

where $Cent_1 = 2/3\ d_2$, $Cent_2 = d_2 + 1/3\ d_3$, $A_1 = (L\ d_2)/2$, $A_2 = (L\ d_3)/2$, $d_2 = TWD - (y_1+d)$, $d_3 = d+y_1 - y_b$, $Cent_3 = y_3/2$,where TWD is the tailwater depth in the stilling basin, y_1 is the gate opening, d is the drop height at the sill, y_b is the height of the endsill, and y_3 is the depth of the river downstream of the stilling basin.

To obtain a bulk average effective depth for the stilling basin and downstream tailwater regions, a weighted mean effective depth is used. An equation for the weighted mean effective depth was developed by (Geldert et al., 1998):

$$d_{eff} = Cent(\exp(1-\frac{\beta X_{1/2}}{L}) + Cent_3(1-\exp(1-\frac{\beta X_{1/2}}{L})) \quad \text{when } \frac{\beta X_{1/2}}{L} \geq 1 \qquad (11)$$

$$d_{eff} = Cent \quad \text{when } \frac{\beta X_{1/2}}{L} < 1 \qquad (12)$$

where β is a constant. Evaluation of β by Geldert et al. (1998) resulted in a value of 2.2. For simplicity the value of β is fixed at 2.2 and is not re-evaluated as parameter fitted to the data. The parameter, $X_{1/2}$, or the effective distance, is discussed bellow.

Effective Distance

Field observations showed that the bubble plume extends further than the length of the stilling basin when the gate opening is sufficient at the tested structures on the Ohio River. Hence the use of the river depth in evaluating the effective depth. The distance the bubbles travel downstream will depend on the discharge and the amount of air entrained in the flow. Based on the above, a representative distance which accounts for the bubble half life, or the distance at which the concentration of air in the flow is half the original value, is determined using the following equation (Geldert et al., 1998):

$$X_{1/2} = -\frac{q}{v_r}\ln(0.5) \qquad (13)$$

where q is the specific discharge and v_r is the rise velocity of the bubbles. The effective distance is used as a representative length up to which a significant amount of gas transfer occurs due to water flowing through the structure.

Site Descriptions

The measurements of methane and oxygen transfer were made at six gated structures on the Ohio River, as depicted in figure 4. The site specific data at each structure during the period of the study are given in table 1. The descriptions for each structure and location are given below from the furthest upstream to the furthest downstream location.

Montgomery Island Lock and Dam is located close to Pittsburgh on the Ohio River (figure 4). It has two fixed 30.5m wide spillways on either side set of 10, 30.5m wide gates. The gates are the lift type as opposed to the tainter gates more common at dams on the Ohio River. Plan view and cross sectional view is shown in Appendix A,

figure 1. Greenup Lock and Dam is located close to Hungtington, West Virginia, on the Ohio River (figure 4). It has a total of 9, 30.5m ft wide tainter gates with the power house on the east bank. A plan view and a cross-sectional view is shown in Appendix A, figure 2 .

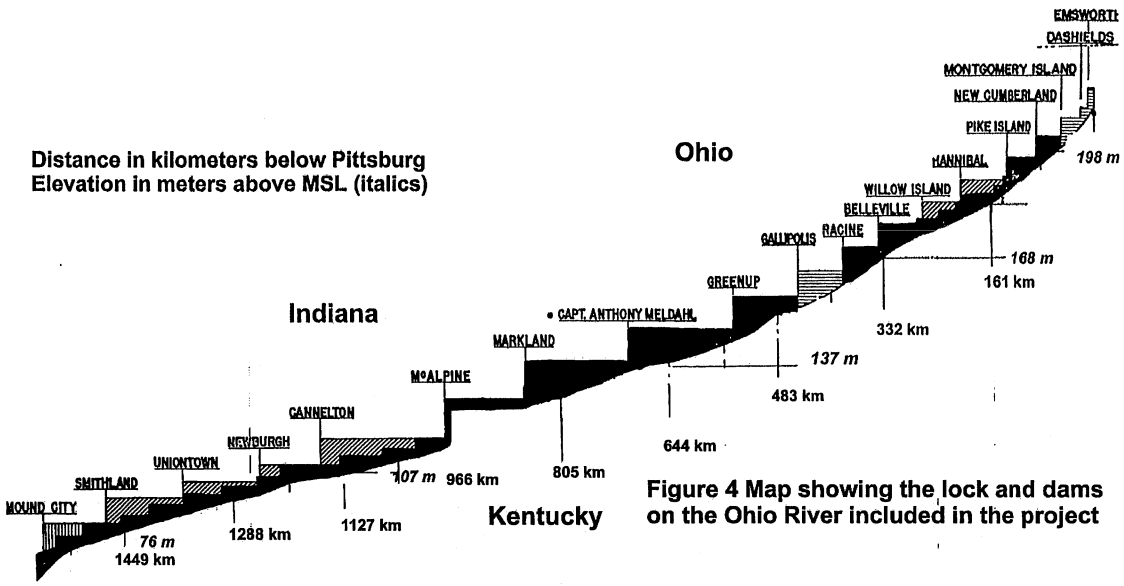

Figure 4. Map showing the lock and dams on the Ohio River included in the project.

Table 1. Site Date for the Six Hydraulic Structures on the Day of Measurements

Elevations, Height, and Length in meters. All elevations are given above MSL.

	Greenup	Markland	Meldhal	McAlpine	Montgomery	Smithland
Date	8/22-23/96	9/1/96	8/24/96	8/26-27/96	8/19/96	8/29/96
Pressure (mmHg)	751	753	753	753	749	757
Head Water Elev	157.3	139.0	148.0	128.0	208.2	98.8
Tailwater Elev.	148.2	128.1	139.2	118.0	202.8	92.4
Sill Elev	146.3	126.5	137.2	122.0	203.4	88.4
Sill Length	11.3	11.3	11.3		9.1	13.1
Stilling Basin Elev	143.6	123.2	134.1	119.2	197.4	80.8
Stilling Basin Length	20.1	21.3	22.9		22.3	24.4
River Bed Elev	142.7	124.4	134.5		197.3	79.3
Trunium Elev	157.6	139.3	148.5			99.8
Bay Width	30.5	30.5	30.5		33.5	33.5
Baffle Block Height	1.8	2.4	1.8		1.5	2.4
End Sill Height	1.2	2.4	1.2		1.2	1.8
Gate Radius	19.5	20.1	19.5			18.9
Sill height	3.0	3.7	4.6		3.0	4.6
Total # Gates	9	12	12	9	10	11
Test Gate	8	7	4	8	5	1

Meldhal Lock and Dam is 702 km below Pittsburgh, close to Portsmouth, on the Ohio River. It has 12, 30.5m wide tainter gates. The special variation at this structures is river bed protection downstream of the end sill. Plan view and cross sectional view is shown in Appendix A, figure 3. Markland Lock and Dam is 855 km below Pittsburgh, located in Switzerland County, Indiana, on the Ohio River. The power house is located on the northern bank. This structure also has river bed protection at the end sill level through gates 1-10. Plan view and cross sectional view is shown in Appendix A, figure 4.

McAlpine Lock and Dam is located at the 977 km mark on the Ohio River. There are two sets of gates; upper and lower. The lower set has 5 gates, 33.5 m ft wide and the upper set has 5 gates 33.5 m wide. A highway bridge crosses ahead of the upper gates. The special characteristic at McAlpine Lock and Dam is the extended apron past the stilling basin in the upper gates, and that the lower pool elevation is lower than the stilling basin elevation. Plan view and cross sectional view is shown in Appendix A, figure 5. Smithland Lock and Dam is located 3.22 km north of the point the Cumberland River joins the Ohio River .It has 11 gates , 33.5 m wide. Plan view and cross sectional view is shown in Appendix A, figure 6.

Sampling Methodology

Four major parties were involved in carrying out these experiments: the U.S. Army Corps of Engineers (Corps), the U.S. Geological Survey, Summit Envirosolutions, and the University of Minnesota. Although each party was present and participated at the sampling site, they had different responsibilities with regard to sample collection, handling, and analysis.

The Corps of Engineers were responsible for coordinating the gate and hydropower gate changes. Approximately ten to fifteen different gate settings were sampled at each structure. The Corps also had to maintain their normal lock operating conditions for daily boat travel, which sometimes resulted in insufficient water for large gate openings because of the low flow rates often experienced in late August on the Ohio River.

The U.S. Geological Survey used two boats, one upstream and one downstream of each structure, to collect water samples for methane analysis using a sampler described below, and to collect data on temperature, pH, conductivity, and dissolved oxygen using a Hydrolab H_2O Probe connected to a Surveyor 3 meter. The upstream boat, shown in figure 4, was sent out first to collect water samples at three different depths at the quarter points of the structure. These samples were used to check for oxygen and methane stratification and lateral variation in concentration. Then each boat, one upstream and one downstream, took measurements at different gate settings, producing eight water samples and six sets of Hydrolab data per gate setting. Figure 5 shows the downstream sampling boat located at the end of the bubble plume roughly 40 m downstream of the gate and 20 m downstream of the stilling basin. Each gate setting was sampled twice (duplicate) and each sample was collected in replicate (two identical samples). This

provided four samples from which sampling and laboratory measurement uncertainties could be evaluated.

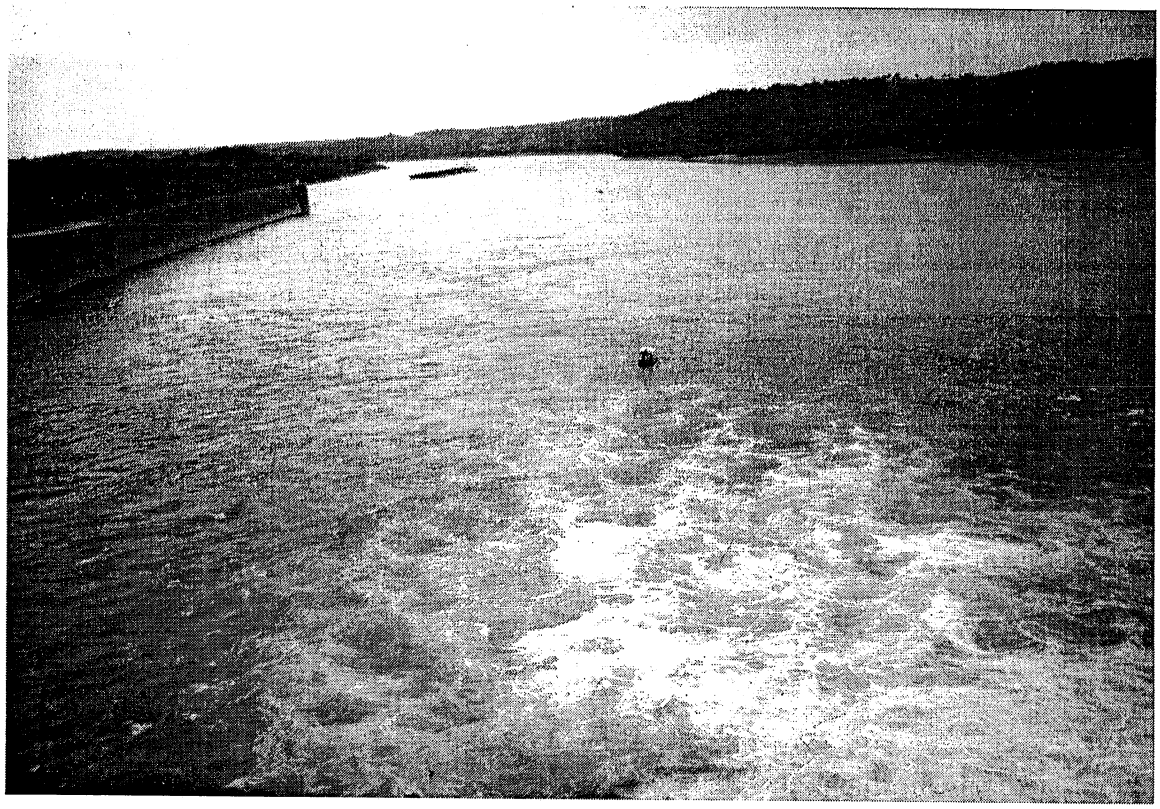

Figure 5. U.S. Geological Survey sampling boat downstream of the structure.

The water samples were then analyzed for methane concentration by Summit Envirosolutions using a headspace analysis technique. Summit's Geoprobe, a large cargo van with a gas chromatograph and various other pieces of scientific equipment, was parked about half a mile from the structure, and samples were brought to them approximately three times a day. The turnaround time provided by the mobile Geoprobe van allowed considerable flexibility in the field effort.

The head space analysis produced methane concentration data that were further analyzed at the St. Anthony Falls Laboratory, University of Minnesota where methane transfer efficiencies were calculated, as well as the effective depth for oxygen transfer, oxygen transfer efficiencies, and measurements uncertainty for both transfer efficiencies.

Description of Sampler

The sampler as shown in Appendix B, was built to function similar to a standard DO sampler. Two Fisher 40 ml Borosilicate glass vials with Teflon faced silicone rubber septa and open top screw caps were used in the sampler. The vials used met EPA specifications and were precleaned, 24 ml, borosilicate glass (Chromatography Research Supplies). Teflon septa were 22 mm diameter PTFE/silicone (Chromatography Research

Supplies). Each vial was numbered with permanent marker and weighed with a fitted screw cap and septa. A line was drawn on each vial near the base indicating the approximate volume of 10 ml of headspace. The sample bottles had to be capped under water to ensure the water in bottles was free of bubbles, and thus had to be built sufficiently large. A detailed description of the sampler is provided in Hibbs and Gulliver (1995).

Sample Analysis for Methane

Headspace Generation

Samples were collected and preserved with formaldehyde as described by McDonald and Gulliver (1992). Samples were weighed full before generation of headspace in the vial. After weighing, a 3-inch long by 0.019-inch outside diameter needle was inserted vertically through the septa with the vial secured in a clamp assembly. The needle was attached to a cylinder of ultra high purity helium and inserted all the way into the vial. A sharpened needle (commonly used for inflating basketballs) was inserted vertically through the septa and into the vial to allow passage of water out of the vial. The removal of approximately 10 ml of sample was regulated by placing a finger over the port of the basketball needle and varying the pressure applied to the opening.

After slightly less than 10 ml of helium was added to the vial, the needle used to supply helium to the vial was removed. The vial was rotated from a vertical to near horizontal position in order to minimize the head of standing water inside the vial. Finger pressure was released on the needle opening to allow any water to escape due to the positive pressure of the headspace inside the vial. After the inside of the vial was equilibrated to near atmospheric pressure, the needle was removed from the vial and septa. The vial was weighed again after headspace generation.

The vial was clamped into a mechanical wrist shaker and vigorously shaken for approximately one minute. The vial was oriented with the septa and cap facing down and the bottom of the vial and headspace facing up. This procedure was employed to eliminate potential loss of methane in the helium headspace through the septa. After headspace equilibration on the shaker, the vials were stored upside down until analysis.

Methane Analysis

Samples were stored with the screw cap and septa down and equilibrated to ambient temperature before analysis. A 250 microliter (μL) gas-tight syringe was used to draw the sample from the headspace of the vial. After removal of one sample of the headspace for injection into the gas chromatograph, an equal volume of water (with no significant dissolved methane) was injected into the vial to replace the removed headspace. Five consecutive sample headspace injections were made into the gas chromatograph for each sample vial.

Sample analysis was completed using a Hewlett Packard Model 5895 Series II gas chromatograph. Injection port configuration was in the splitless mode. The column used

was a Alltech Part No. 85501PC packed column with a stationary phase consisting of 0.19 percent picric acid on graphpac. Sample detection was accomplished using a flame ionization detector (FID). Chromatographic conditions included an injection port temperature of 250°C; detector temperature of 300°C; column temperature of 90°C; and a carrier gas flow rate of approximately 30 ml/minute. The oven was ramped to 120°C for 5 minutes after each group of samples were analyzed to stabilize the baseline. The hydrogen flow rate to the FID was approximately 30 ml/minute and the air flow rate was set at approximately 400 ml/minute. The resulting retention time for methane was approximately 0.38 minutes.

An initial study was performed to verify a linear response for the method and detector. After the initial verification of linearity, a mid-point calibration standard was used daily to generate a response factor.

Methane Quantification

Methane concentrations in each of the water samples was quantified using a certified gas standard obtained from Scott Specialty Gases. The standard concentration was 1,027 parts per million (volume/volume) in a balance of nitrogen. The standard was certified to $\pm$ 2 percent by the manufacturer. Sample concentrations were calculated by first quantifying the concentration of methane in the vial headspace:

$$C_{HS} = \frac{RF * A_S * 1000}{V_{inj}} \tag{14}$$

where C_{HS} is concentration of methane in the sample headspace (µg methane/liter headspace), RF is response factor for the methane standard (µg/unit area), A_S is area of the GC peak for the unknown sample (unit area), V_{INJ} is volume of the unknown sample headspace injected (L).

Methane concentrations in the water samples were calculated using the following equation:

$$C_W = C_{HS}\left(\frac{V_{HS}}{V_w} + \frac{1}{H_{LC}}\right) \tag{15}$$

where, C_W is concentration of methane in the water sample, C_{HS} is concentration of methane in the sample headspace (µg methane/liter headspace), V_{HS} is volume of headspace in the equilibrated sample bottle, V_W is volume of water in the equilibrated sample bottle, and H_{LC} = Henry's Law constant for methane (dimensionless)

Instrument Calibration and Quality Assurance/Quality Control

An initial study was performed to verify the linearity between detector response and mass methane injection (Thene and Gulliver 1990) and determine whether there was a significant intercept. Dilution of the standard was made using a 500 ml glass sampling bulb and a four point calibration curve was generated. For each point of the calibration curve 10 injections were made and the standard areas were averaged. Standard deviations

for the lowest concentration standards (approximately 0.0003 µg methane and 0.001 µg methane) were 434 and 331 area counts, respectively. Although the response was generally linear, there was a small but significant intercept which was considered in the determination of methane concentration.

The limit of detection (LOD) and limit of quantification (LOQ) for the method were calculated using the average standard deviations for the two lowest methane standard dilutions from the linearity study. The LOD and LOQ were defined by the following equations:

$$\text{LOD} = 3 \text{ x (standard deviation)} \quad (16)$$

$$\text{LOQ} = 10 \text{ x (standard deviation).} \quad (17)$$

Based on an average standard deviation for the two standards (383 area counts) the calculated LOD was 0.31 µg/L and the LOQ was 1.0 µg/L. These values were generated by inserting area count values of 1148 (3 x standard deviation) and 3,830 (10 x standard deviation) into a spreadsheet used to calculate methane concentrations for the project.

UNCERTAINTY ANALYSIS

The measurement uncertainty which occurs due to instrument error, operator error, and sampling assumptions was calculated using a standard first order, second moment analysis. The two main components of this analysis are precision uncertainty and bias uncertainty (Abernathy, et al 1985)

$$U_M^2 = U_p^2 + U_B^2 \tag{18}$$

where U_M is the measurement uncertainty, U_P is the precision uncertainty, and U_B is bias uncertainty. The bias uncertainty can further be divided into these parts (Thene and Gulliver 1990):

$$U_B^2 = U_{HCF}^2 + U_{EH}^2 + U_{cal}^2 \tag{19}$$

where U_{HCF} is the uncertainty in the headspace correction factor, U_{EH} is the uncertainty in the bias of the Henry's Law constant, and U_{cal} is the calibration uncertainty.

When calculating the measurement uncertainty for the data collected, it was clear that the bias uncertainty, calculated in equation 19, was negligible compared to the precision uncertainty as found by Thene and Gulliver(1990). Therefore the measurement uncertainty for the data collected is said to be equal to the precision uncertainty.

The one exception is the bias created by the upstream lateral variation in concentration. This sampling uncertainty can in some circumstances be an important source of bias in the measurements. In the calculation of transfer efficiencies, it is assumed that the samples taken upstream of the structure represent an average concentration of the methane concentration flowing past the structure. There were at least two sets of samples taken from each gate setting. If the lateral variation in the methane concentration is significant, even though two sets of samples are taken, the upstream samples may not be representative of the horizontal variation in concentration that can occur. Down stream of the structure there is intense mixing and sampling uncertainty is not considered to be a potential problem. The method followed to account for the sampling uncertainty in the upstream measurements is discussed under the section on sampling uncertainty.

Elimination of Outliers

As described in the methodology, five injections were made to the gas chromatograph from each bottle. Four bottles were sampled from each location, which results in a total of twenty injections to the gas chromatograph for analysis from each location.

The outliers within each bottle were evaluated using the mean concentration and the precision uncertainty for the five injections from each bottle :

$$U_p = t_{n-1} * \sigma_n \tag{20}$$

where U_p is the precision uncertainty adjusted to the 95 % confidence interval, t_{n-1} is the Student's t score, σ_n is the standard deviation of the injection concentration, and n is the number of injections (n=5). All the values outside the mean $\pm U$ limit were discarded and a new mean and a standard deviation was calculated.

Uncertainty in Bottle Concentration

In order to incorporate the two sets of samples taken from each point, it was decided that the most representative analysis would be to calculate the measurement uncertainty by lumping all the samples together for each measurement condition as follows:

$$U_m = t_{n-1} * \frac{\sigma_n}{\sqrt{n}} \tag{21}$$

where U_m is the uncertainty of the four bottle mean concentration, σ_n is the standard deviation of all the samples and n is the number of injections (n=20).

Sampling Uncertainty

As mentioned before, when there is significant horizontal variation in the concentration in the upstream reservoir, sampling uncertainty becomes an important consideration. It is difficult to account for the actual horizontal variation at the time of sampling when only one gate is in operation. Therefore a method is needed to account for the sampling uncertainty based on the variation of the sample taken.

An explanation as to how lateral variation in concentration might cause errors in the computed transfer efficiency at such structures is that the water sampled by the upstream boat was different to the flow going through the gate. This can result due to the fact that only one gate was in operation.. When lateral variation in concentration occurs, such as show in figure 6, if the boat positioned to the left would sample a lower methane concentration. Whereas if the boat was positioned more to the right it would sample a higher concentration. The water flowing through the gate into the stilling basin is well mixed and the down stream boat would sample close to mean concentration.

Assuming that the concentration of methane at each location along the structure remains constant with time, then the variation of the methane concentration at the sampling point with time would represent the error caused by the horizontal variation in methane. This is based on the idea that the sample variation is caused by sampling different blocks of water flowing in from different parts of the reservoir, and not by the change in methane concentration at one location with time. Then the variation of the methane concentration at the sampling point with time is actually due to spatial variation.

The result is a time reference being used to represent the horizontal concentration gradient along the structure.

With the above assumption, the standard error resulting from a linear regression of the change in concentration with time will represent the standard deviation of the samples as caused by the spatial variation. Therefore, the sampling uncertainty caused by the horizontal variation in methane concentration in the upstream pool is given by:

$$U_s = S_e \times t_{n-1} \tag{22}$$

where S_e is the standard error from the regression analysis and n is the number of upstream samples.

Then the uncertainty in the upstream concentration accounting for the sampling uncertainty Umu would be given by the equation:

$$U_{mu}^2 = U_m^2 + U_s^2 \tag{23}$$

where Um is the measurement uncertainty in the bottle calculated using equation 21 and Us is the sampling uncertainty determined from equation 22 for the upstream samples.

Uncertainty in the Transfer Efficiency

The uncertainty in the transfer efficiency due to the precision uncertainty in the measurements is calculated as follows:

$$U_E^2 = \left(\frac{C_d}{C_u^2} * U_{mu}\right)^2 + \left(\frac{-1}{C_u} * U_{md}\right)^2 \tag{24}$$

where U_E is the uncertainty in the transfer efficiency, U_{mu} is the uncertainty in the upstream concentration calculated using equation 21, U_{md} is the uncertainty in the downstream concentration calculated using equation 21, C_d is the concentration downstream, and C_u is the concentration upstream.

Uncertainty in the Dissolved Oxygen Measurement

Oxygen was measured as a percent of the saturation at local atmospheric pressure. Three measurements were taken with a field probe , one each at three different depths. The uncertainty of the measured oxygen is calculated as follows:

$$U_x = t_{n-1} * \frac{\sigma_x}{\sqrt{n}} \tag{25}$$

where U_x is the uncertainty in the measured oxygen percent saturation, σ_x is the standard deviation of the oxygen measurements based on the three different depths, n is the number of samples (n=3).

Uncertainty in the Predicted Dissolved Oxygen Concentration

As mentioned before, a downstream percent saturation of oxygen is calculated based on the converted transfer efficiency of methane, the upstream percent saturation, and the effective saturation concentration. The uncertainty in the predicted DO value is calculated as follows:

$$U_{Xd}^2 = \left\{\left(100 * \frac{C_{se}}{C_s} - X_u\right) * U_{Eo}\right\}^2 + \left\{(1 - E_{oi}) * U_{Xu}\right\}^2 \qquad (26)$$

where X_u is the percent saturation oxygen upstream, X_d is the percent saturation oxygen downstream, U_{xu} is the uncertainty in the DO percent saturation upstream calculated using equation 21, and U_{Eo} the uncertainty in the indexed oxygen efficiency calculated as follows:

$$U_{Eo} = \frac{1}{f_i} * (1 - E_M)^{\frac{(1-f_i)}{f_i}} * U_E \qquad (27)$$

where E_M , f_i , and U_E have been previously defined.

RESULTS AND DISCUSSION

Four measurements of dissolved gas concentrations were made at each hydraulic structure; upstream methane and oxygen percent of saturation and downstream methane and oxygen percent of saturation. As mentioned in the uncertainty analysis, a linear regression was done on the upstream concentrations to account for the bias introduced to the measurements due to possible lateral variation in the concentration in the upstream pool. Therefore, the upstream concentration to calculate the transfer efficiency was taken from the regression curve as shown in figure 6. The effective saturation concentration used to determine oxygen transfer efficiency was calculated using the effective depth in the plunge pool.

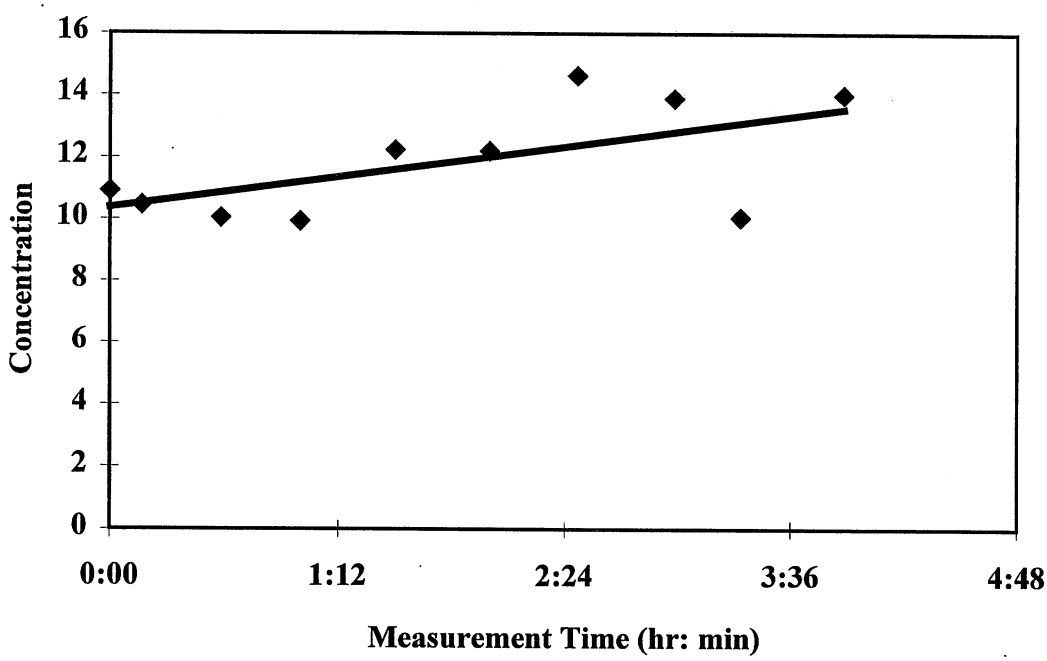

Figure 6. Regression fit for upstream methane concentration at Markland Lock and Dam.

Accounting for the bias due to lateral variation in concentration in the upstream pool showed a significant increase in the calculated uncertainty for methane transfer at Markland L/D while the calculated uncertainties showed a smaller increase at Meldhal L/D and very little change at Greenup L/D. Upstream methane measurements at Markland L/D showed significant lateral variation(Appendix C). The methane samples taken upstream at Greenup L/D showed insignificant lateral variation relative to the measurement uncertainties.

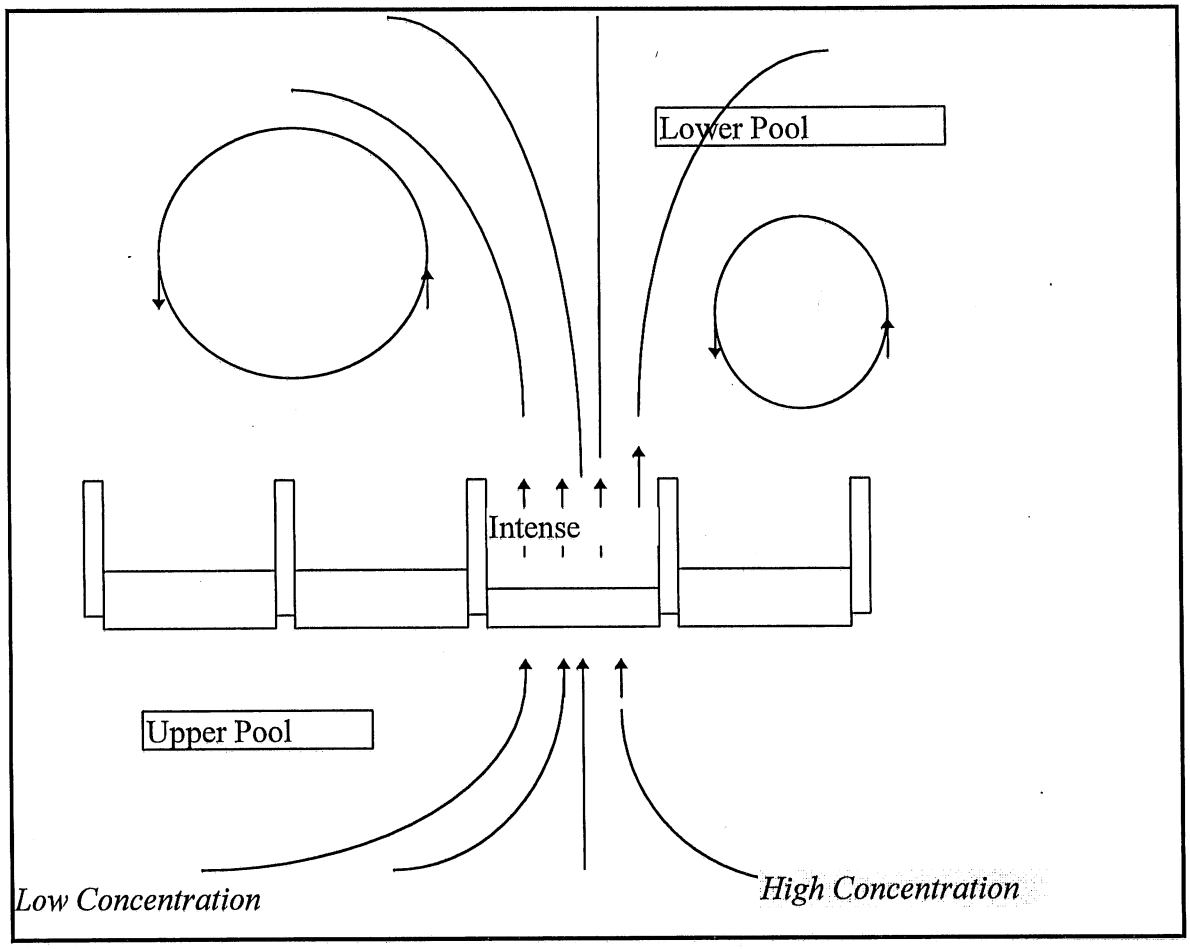

Figure 7. Flow field close to the gate and lateral variation in upstream gas concentration.

Analysis of the methane transfer data at the tested structures reveal the complexity of the hydraulics and gas transfer at lock and dam (L/D) structures. From figure 8, which shows methane and oxygen transfer efficiency for the gated sill at Greenup L/D, it is clear that methane transfer is low at small gate openings, and has a significant increase at roughly a 2.5 ft gate opening to a plateau of approximately 30% at higher discharges. This is the typical trend for gas transfer at submerged gated sills where gas transfer increases significantly with discharge after a hydraulic jump forms at the free surface. The oxygen sampled at Greenup L/D show significant stratification with depth . As a result of the large vertical variation in dissolved oxygen in the upper pool, the calculated oxygen transfer efficiencies do not show a clear trend as seen in the methane data, and have large measurement uncertainties. The high dissolved oxygen levels at the intake surface bias the upstream percent saturation for oxygen. The water flowing through the gate will have a lower mean dissolved oxygen concentration. Therefore, the gas transfer efficiency calculated would show much lower than actual values.

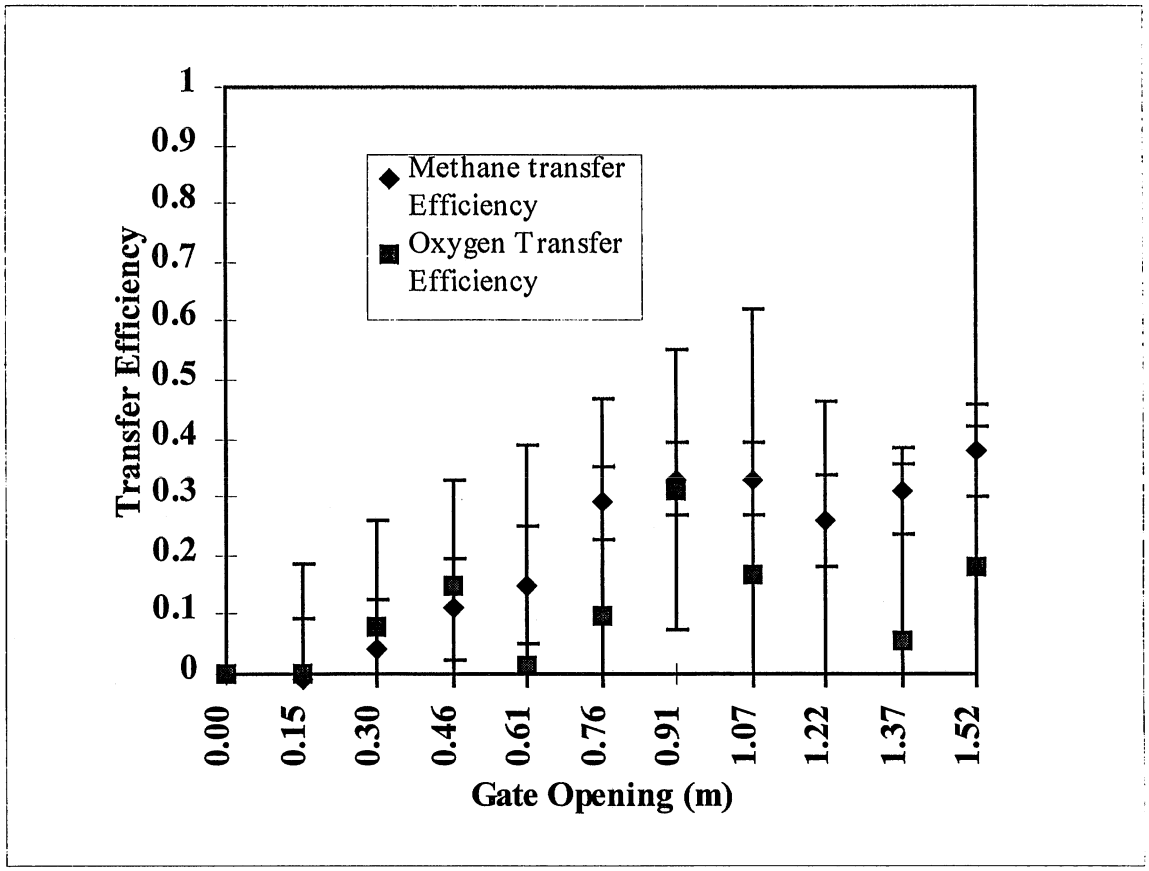

Figure 8. Gas transfer efficiency at Greenup Lock and Dam. Vertical bars represent computed measurement uncertainty to the 95% confidence level.

Similar plots of methane transfer efficiency at Markland and Meldhal L/D shown in figures 9 and 10, indicate a significant measurement uncertainty, contrary to the methane measurements at Greenup L/D. A strong lateral gradient in methane concentration in the upper pool at Markland L/D could bias the results . As discussed, large variations in concentration in the upper pool can result in significant sampling uncertainty, which increases the overall uncertainty calculated for the transfer efficiency as seen in figures 9 and 10. In fact, the uncertainties in the concentration are sufficiently large that the assumptions implied in the first order second moment analysis, i.e. that the measured value is much larger than the associated uncertainty, are violated (Kline 1985).

Dissolved oxygen at Markland and Meldhal L/Ds were not stratified. In addition, the upstream concentration deficit was large enough to have a relatively small uncertainty for the calculated transfer efficiency. This result is indicative of the advantages of the dual dissolved gas measurement at large hydraulic structures. Once the field crews are mobilized, the additional effort required to measure methane transfer is not that significant. The added advantages are two fold; 1) It is less likely that both measurements will have a high uncertainty, 2) The transfer efficiency of each gas

provides an independent verification of the measurements that can serve as a test for unknown measurement uncertainty, such as at Meldhal L/D

Based on the structural and hydraulic similarities between Greenup, Markland and Meldhal L/D s, it is safe to say that at Markland and Meldhal L/Ds, similar trends in gas transfer should occur as shown by the transfer efficiencies calculated based on the oxygen samples taken concurrently with the methane samples at these structures (figures 9 and 10. This is further supported by the previous work by Pruel and Holler (1969) which found gas transfer characteristics at Markland and Meldhal L/Ds to be very similar to that shown by the methane transfer results at Greenup L/D. Thus the methane measurements will be used to indicate gas transfer efficiency at Greenup L/D, while the oxygen measurements will be used to indicate gas transfer efficiency at Markland and Meldhal L/Ds.

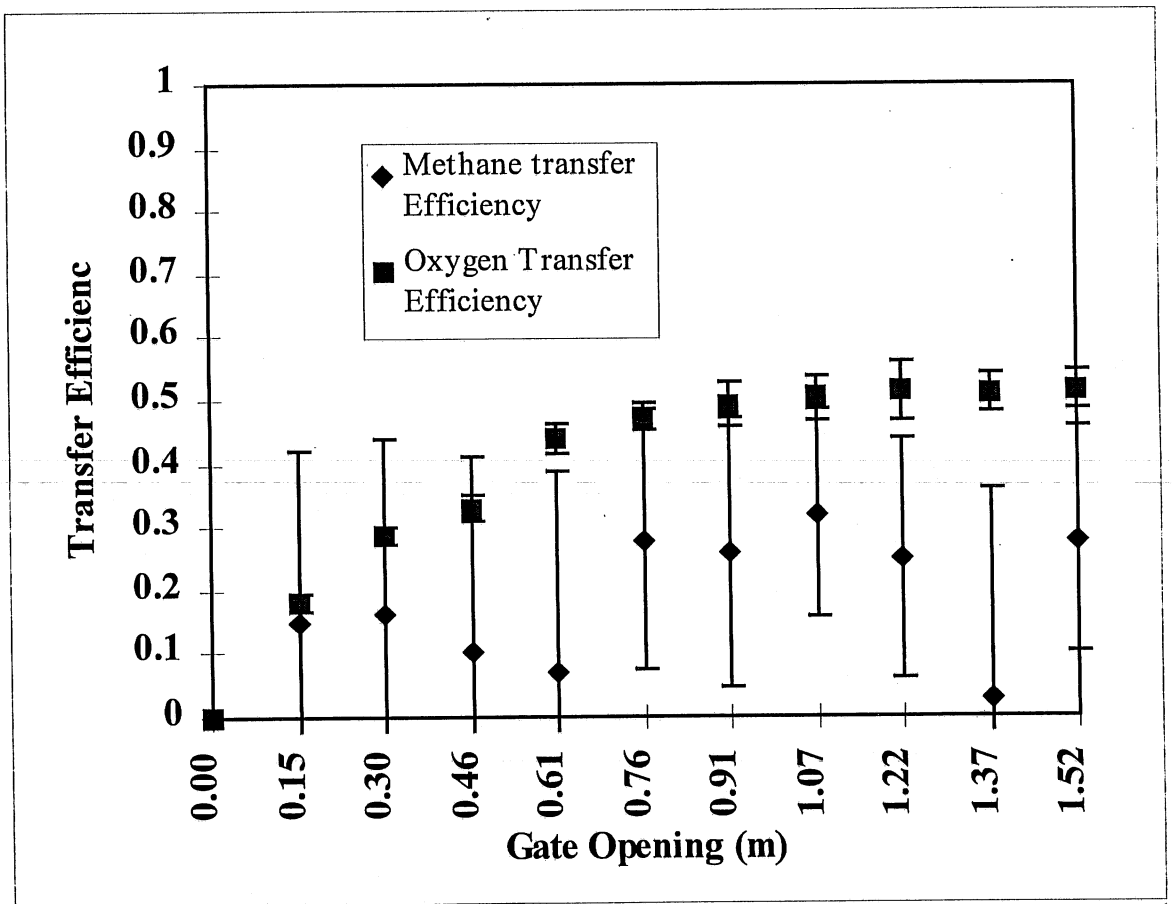

Figure 9. Gas transfer efficiency at Markland Lock and Dam. Vertical bars represent computed measurement uncertainty to the 95% confidence level.

Smithland lock and Dam structure has a high level of submergence (10-13 feet compared to 4-6 feet) compared with the rest of the gated sill structures. The high submergence prevents a hydraulic jump from forming on the free surface for the discharges tested. Hence, air entrainment is low and results in small gas transfer efficiencies as shown in figure 11. Oxygen data for the above structures show minimal changes between the upper pool and lower pool percent saturation values, which correspond well to the methane analysis.

At Montgomery L/D, the flow characteristics are different as a result of the stepped spillway and the unsubmerged sill. The discharge is a typical nappe jet, impinging on the lower pool at roughly 9 m/s and a small impact angle. Transfer efficiency for methane show trends that are typical of a nappe jet (Avery and Novak 1978) with high gas transfer at lower gate openings as a result of the high energy and entrainment of air into the jet. Gas transfer efficiency decreases with gate opening as the thickness of the jet increases. The oxygen data at Montgomery L/D is similar to Greenup Lock and Dam with significant vertical stratification in the upper pool and a significant uncertainty in transfer efficiencies.

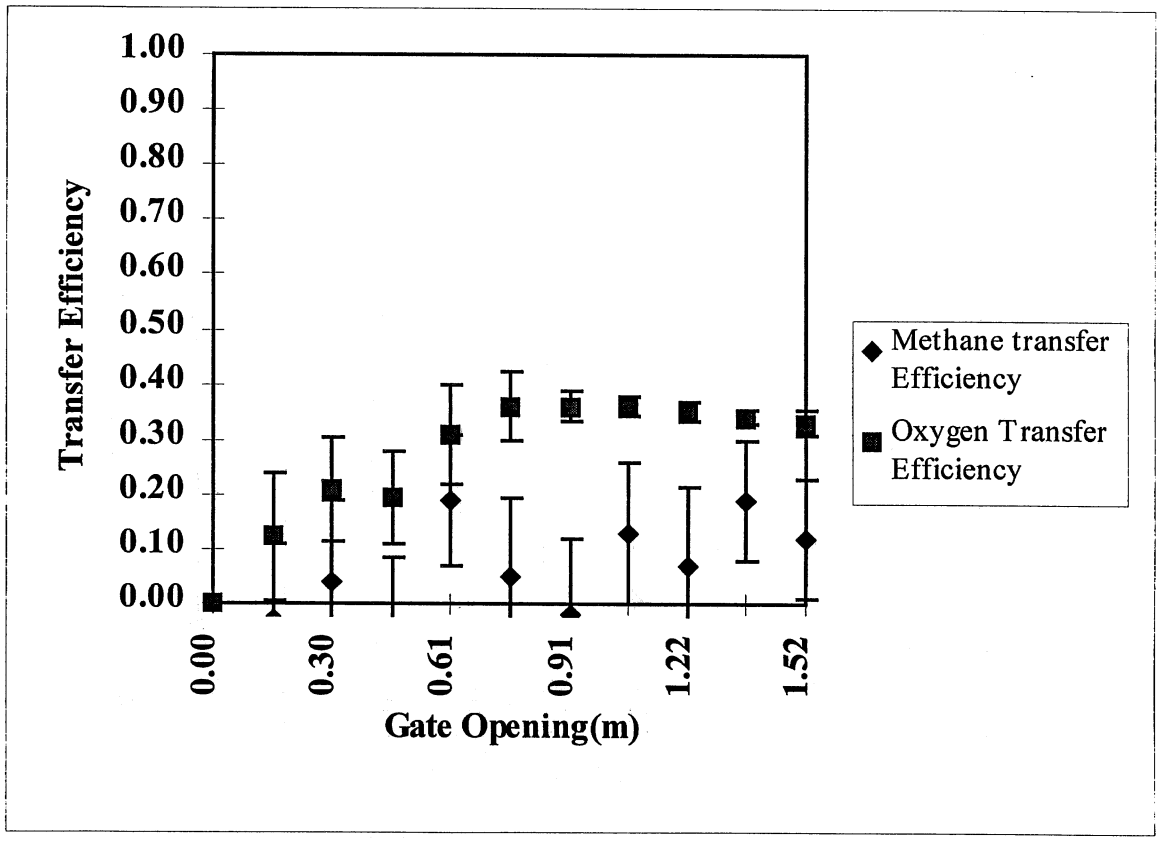

Figure 10. Gas transfer efficiency at Meldahl Lock and Dam. Vertical bars represent computed measurement uncertainty to the 95% confidence level.

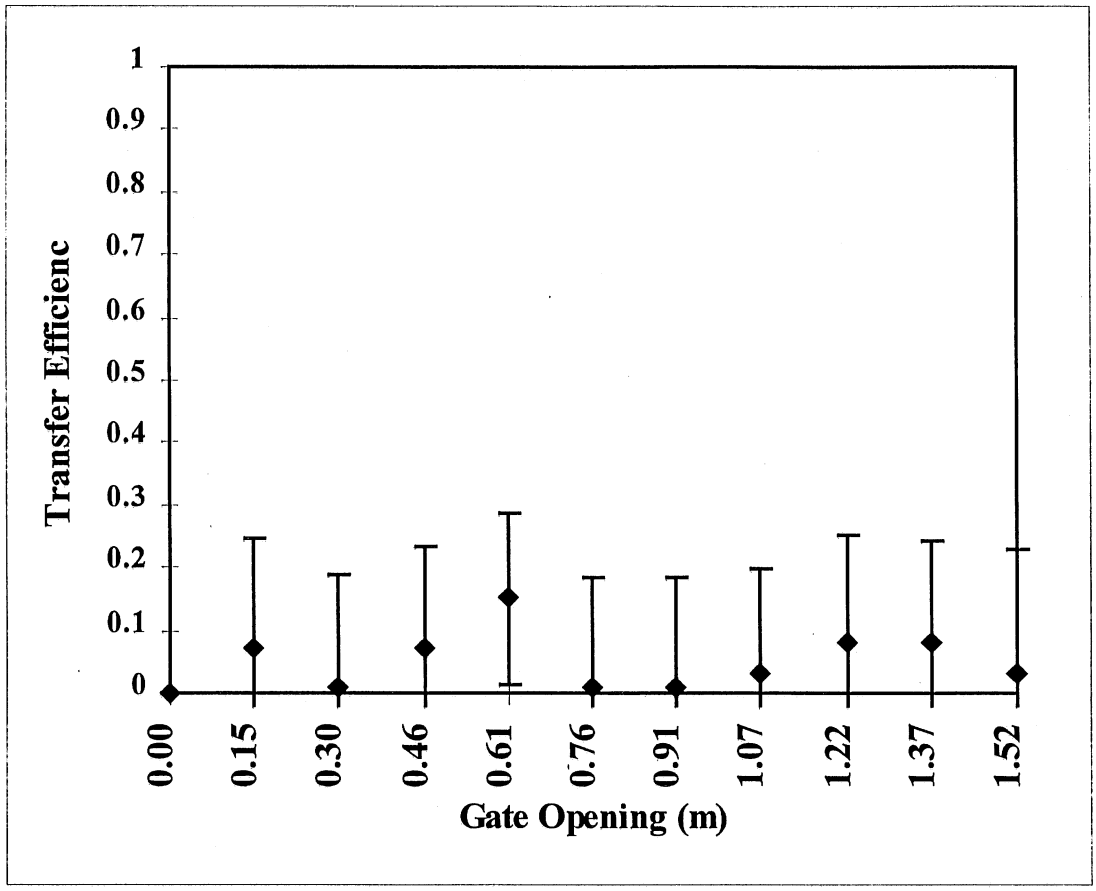

Figure 11. Gas transfer efficiency at Smithland Lock and Dam. Vertical bars represent computed measurement uncertainty to the 95% confidence level.

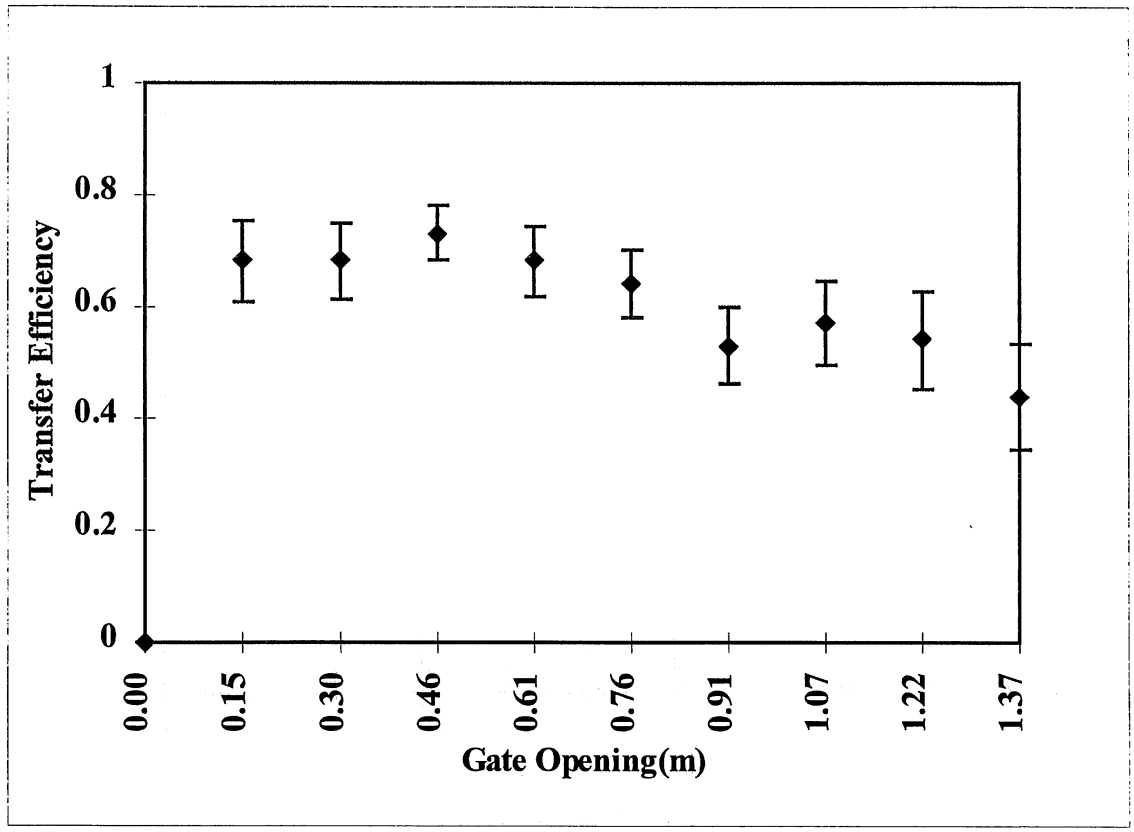

Figure 12. Gas transfer efficiency at Montgomery Island Lock and Dam. Vertical bars represent computed measurement uncertainty to the 95% confidence level.

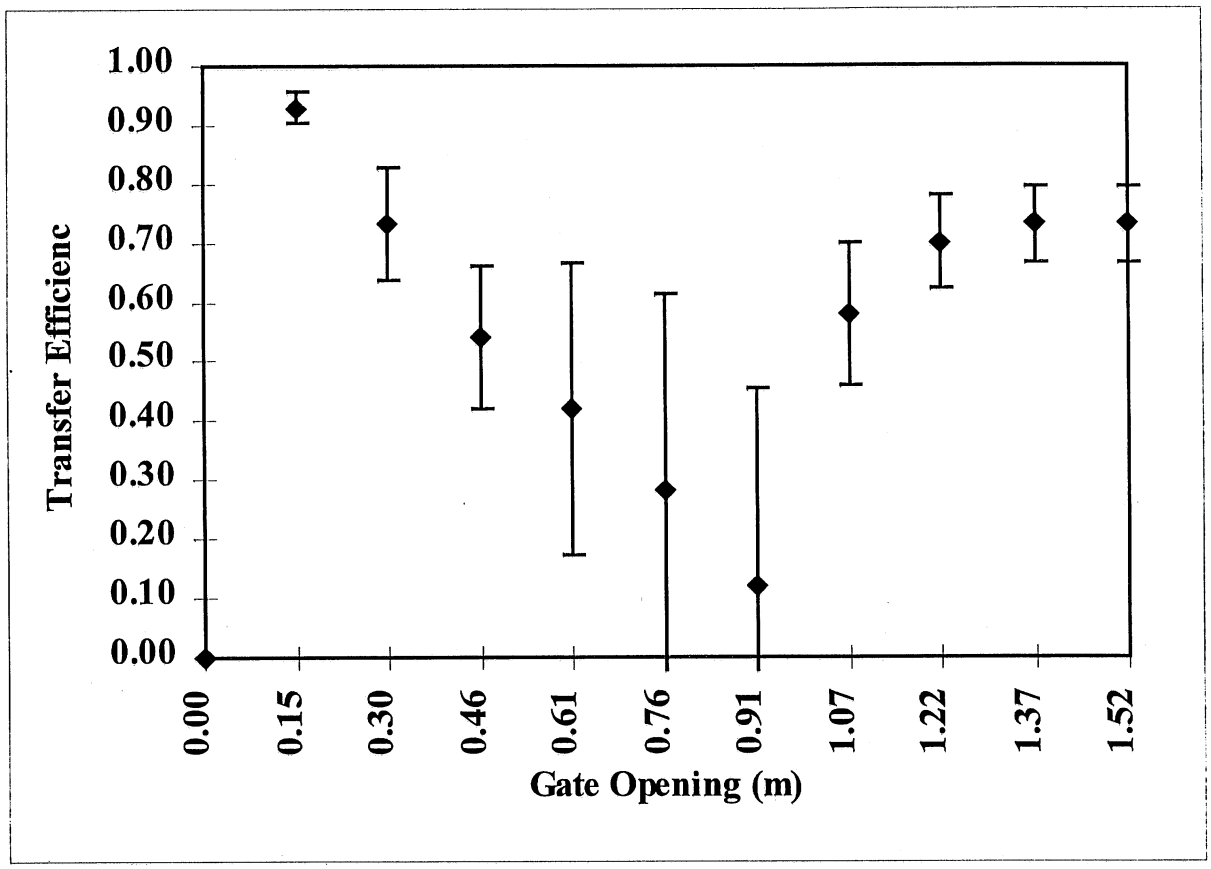

Figure 13. Gas transfer efficiency at McAlpine Lock and Dam. Vertical bars represent computed measurement uncertainty to the 95% confidence level.

McAlpine L/D is a special case among the gates tested. The Significant difference is that the tailwater level is below the stilling basin at both sets of gates. The variation in methane concentration in the upper pool (Appendix C) as seen at Markland prevents drawing clear conclusions regarding the methane transfer characteristics at McAlpine L/D. Speculation as to how the flow behaves at the lower gates would result in a weir type flow when the water flows along the stilling basin and falls from the endsill to the tailwater. Initially , relatively large amounts of air can get entrained in the water as it flows along the stilling basin which could result in high transfer efficiencies at small gate openings. At larger gate openings, the initial entrainment reduces as the depth of water increase and the weir type flow over the endsill would dominate gas transfer. The upper set of gates have a long apron that extends past the stilling basin which enables high air entrainment into the flow as a result of the fully developed boundary layer which results on the apron. The drop at the end sill is not as high as in the lower set of gates to result in significant gas transfer.

Table 2. Gas Transfer across Markland Hydropower Facility

Gate Setting (%)	Location (Upstream/downstream)	Oxygen Saturation (Percent)	Methane Concentration (mg/L)
100 all	down	79.25	14.08
	up	79.4	17.2
90,100,90	down	79.55	17.65
	up	79.73	17.87
80,70,70	down	79.27	19.51
	up	79.63	22.65
100,90,90	down	78.95	15.6
	up	79.03	16.63
90,90,100	down	79.65	25.13
	up	80.43	34.74
70,80,70	down	80.05	19.88
	up	79.83	34.32
70,70,80	down	80.75	22.15
	up	80.47	31.49

Methane transfer data and upstream and downstream dissolved oxygen data collected at the hydropower facilities associated with the Markland L/D structures is given table 2. The results of the methane transfer measurements across the hydropower turbines at Markland L/D does not provide reliable results. Analysis of the data collected at Markland L/D does not show a trend and has unexpectedly high amounts of methane transfer. The variation in the transfer efficiency can clearly be related to the change in the upper pool methane concentration. Similarly, the data for the hydropower facility at Greenup L/D show expectedly low transfer when the upstream methane concentration remains constant and show high values when the upper pool concentration varies. Analysis of the oxygen data at Markland L/D results in gas transfer values in the expected range for transfer across hydropower turbines. Unfortunately, the oxygen data at Greenup L/D is unreliable to provide a clear picture of the gas transfer characteristics across that facility.

It seems a coincident that, at tested structures for which the oxygen data does not provide useful information, the methane data works well. While at structures where the methane data is unreliable the oxygen data provides sufficient data on gas transfer across these hydraulic structures. The methane tracer technique works well when there is no horizontal variation in methane concentration in the upper pool. Due to small measurement uncertainties, and the lack of supersaturation effects such as in oxygen transfer, the methane racer provides detailed information on the gas transfer characteristics at hydraulic structures. Therefore, it is prudent to take methane and oxygen samples simultaneously when measuring gas transfer across hydraulic structures.

CONCLUSIONS

Gas transfer at six hydraulic structures on the Ohio River was measured using naturally occurring methane as a tracer and direct dissolved oxygen measurements. Both upstream stratification and the high concentrations of DO in the reservoir often result in very large measurement uncertainty for oxygen transfer at large hydraulic structures. Also, the lateral variation in concentration in the upstream pool significantly affects gas transfer measurements at such structures. Considering the field mobilization costs for sampling large river-reservoir systems, it is prudent to incorporate both methane and oxygen sampling into gas transfer measurement program.

The following observations have been made based on the results of these measurements:

- A submerged hydraulic jump below a gated structure produces minimal oxygen transfer except when the jump is close to forming.
- An unsubmerged hydraulic jump results in oxygen transfer efficiency between 30-50 percent. Thus the oxygen added to the water passing through the structures is between 30-50 percent of the difference between the upstream concentration and the local equilibrium concentration
- Water falling over a weir can have transfer efficiency ranging from 50 to 80 percent.
- Gas transfer across hydropower facilities is minimal.

REFERENCES

Abernathy, R. B., Benedict, R. P., and Dowell, R.B. (1985). "ASME Measurement Uncertainty." *J. Fluids Engrg.*, 107(2), 161-164.

Geldert, D.A., Gulliver, J. S., Wilhelms, S. (1998). "Modelling Dissolved Gas Supersaturation Below Spillways: Plunge pools, " *Jour. of Hydraulic Engrg.*

Gulliver, J. S., Hibbs, D. E., McDonald, J. P. (1997). "Measurement of Effective Saturation Concentration for Gas Transfer," *J. Hydr. Engrg*, 123(2)

Gulliver, J. S.,Thene, J. R, Rindels, A. J. (1990). "Indexing Gas Transfer in Self Aerated Flow," *J of Envir. Engrg*, 116(3), 503-523.

Gulliver, J. S and Wilhlems, S. C. (1992). "Discussion of 'Aeration at Ohio River Basin Navigation Dams' by S.F Railsback, J.M Bownds, M.J Sak, M.M Stevens, and G.H. Taylor," *J. Envir. Engrg*, 108(3), 444-446.

Hibbs, D. E. and Gulliver, J. S. (1995). "Prediction of Dissolved Gas Supersaturation Below Spillways,"*Proceedings, Water Power '95,* ASCE, New York, NY.

Hoyt, J. W. and Selin, R.H.J. (1989). "Hydraulic Jump as Mixing Layer," *J. Hydr. Engrg*, 115(12), 1607-1613.

Kline S. J. (1985). "The Purpose of Uncertainty Analysis," *J. of Fluids Engrg,* 107,153-158.

Kissel, P. C. and Ribbins, A. I. (1991). "Overcoming Anti Hydro Policies in the Ohio River Basin," *Hydro Review*, 10(1), 19-27.

McDonald, J. P. and Gulliver, J. S. (1992). "Methane Tracer Technique for Gas Transfer at Hydraulic Structures," *Project No. 325*, St. Anthony Fall Hydraulic Laboratory, University of Minnesota, Minneapolis, Minnesota.

Preul, H. G. and Holler, A. G. (1969). "Reaeration Through Low Head Dams in the Ohio River," *Proceedings of the Industrial Waste Conference*, May 6-8 ,1969, Purdue University, South Bend, IN, 1249-1270.

Thene, J. R. and Gulliver, J. S. (1990). "Gas Transfer Measurements Using Headspace Analysis of Propane," *J Envir. Engrg*, 116(6), 1107-1123.

Thene, J. R. and Gulliver, J. S. (1989). "Gas Transfer at Weirs Using the Hydrocarbon Gas Tracer Method with Headspace Analysis," *Project Report No 273*, St. Anthony Falls Hydraulic Laboratory, University of Minnesota, Minneapolis, MN.

Sales M.J and Railsback S.F., (1991). "A new Look at Environmental Mitigation Practices," *Hydro Review*, 10(4), 58-66.

Appendix A

Site Description

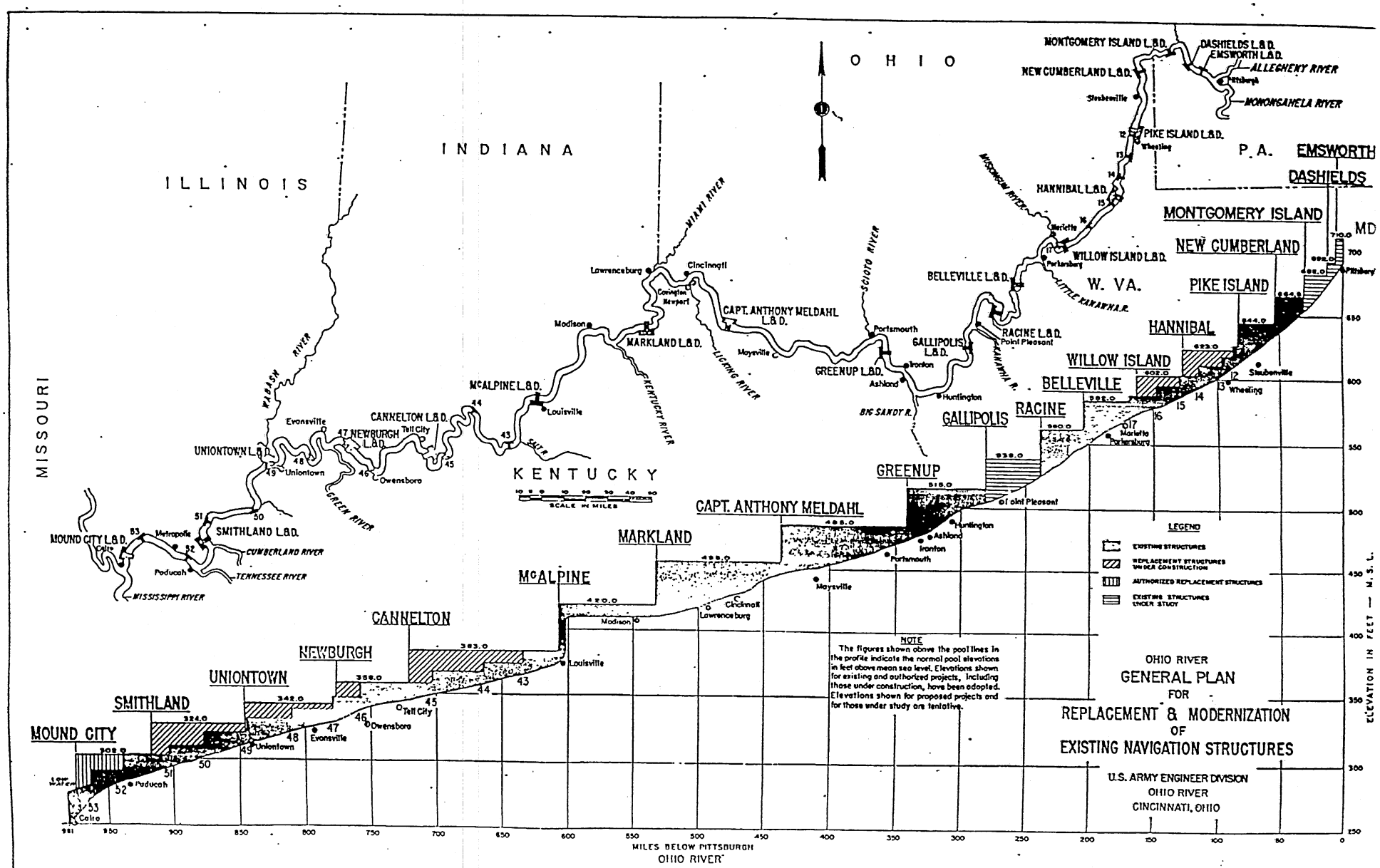
ILLINOIS
INDIANA
OHIO
KENTUCKY
W. VA.
P.A.
MD
MISSOURI
WABASH RIVER
GREEN RIVER
CUMBERLAND RIVER
TENNESSEE RIVER
MISSISSIPPI RIVER
MIAMI RIVER
LICKING RIVER
KENTUCKY RIVER
SCIOTO RIVER
BIG SANDY R.
KANAWHA R.
MISSOURI RIVER
LITTLE KANAWHA R.
ALLEGHENY RIVER
MONONGAHELA RIVER
MOUND CITY L&D.
SMITHLAND L&D.
UNIONTOWN L&D.
NEWBURGH L&D.
CANNELTON L&D.
McALPINE L&D.
MARKLAND L&D.
CAPT. ANTHONY MELDAHL L&D.
GREENUP L&D.
GALLIPOLIS L&D.
RACINE L&D.
BELLEVILLE L&D.
WILLOW ISLAND L&D.
HANNIBAL L&D.
PIKE ISLAND L&D.
NEW CUMBERLAND L&D.
MONTGOMERY ISLAND L&D.
DASHIELDS L&D.
EMSWORTH L&D.
Cairo
Metropolis
Paducah
Evansville
Tell City
Owensboro
Louisville
Madison
Lawrenceburg
Cincinnati
Covington
Newport
Maysville
Portsmouth
Ironton
Ashland
Huntington
Point Pleasant
Parkersburg
Marietta
Wheeling
Steubenville
Pittsburgh
SCALE IN MILES
MILES BELOW PITTSBURGH
OHIO RIVER
ELEVATION IN FEET — M.S.L.
LEGEND
EXISTING STRUCTURES
REPLACEMENT STRUCTURES UNDER CONSTRUCTION
AUTHORIZED REPLACEMENT STRUCTURES
EXISTING STRUCTURES UNDER STUDY
NOTE
The figures shown above the pool lines in the profile indicate the normal pool elevations in feet above mean sea level. Elevations shown for existing and authorized projects, including those under construction, have been adopted. Elevations shown for proposed projects and for those under study are tentative.
OHIO RIVER
GENERAL PLAN
FOR
REPLACEMENT & MODERNIZATION
OF
EXISTING NAVIGATION STRUCTURES
U.S. ARMY ENGINEER DIVISION
OHIO RIVER
CINCINNATI, OHIO

Figure 1

Site Data
Hydraulic Structures (Ohio River)

	Belleville	Greenup	Markland	Meldhal	McAlpine	Montgomery	Smithland
Date	20,21/8/96	22,23/8/96	1/9/96	24/8/96	26,27/8/96	19/8/96	29/8/96
Pressure (mmHg)	751	751	753	753	753	749	757
Temperature (deg C)							
Head Water Ele	582.4	515.9	455.8	485.6	420	682.9	324
Tailwater Ele	560.6	486.2	420.1	456.55	387	665.2	303
Sill Ele	550	480	415	450	400	667	290
Sill Length	37	37	37	37		30	43
Stilling Basin Ele	537	471	404	440	391	647.5	265
Stilling Basin Lenght	80.75	66	70	75		73	80
River Bed Ele	557	468	408	441		647	260
Truniun Ele	594	517	457	487		n/a	327.25
Bay Width	110	100	100	100		110	110
Baffle Block Height	6	6	8	6		5	8
End Sill Height	4	4	8	4		4	6
Gate Radius	64	64	66	64		n/a	62
Sill height	13	10	12	15		10	15
Total # of Gates	8	9	12	12	9	10	11
Test Gate	6	8	7	4	8	5	1

Table 1

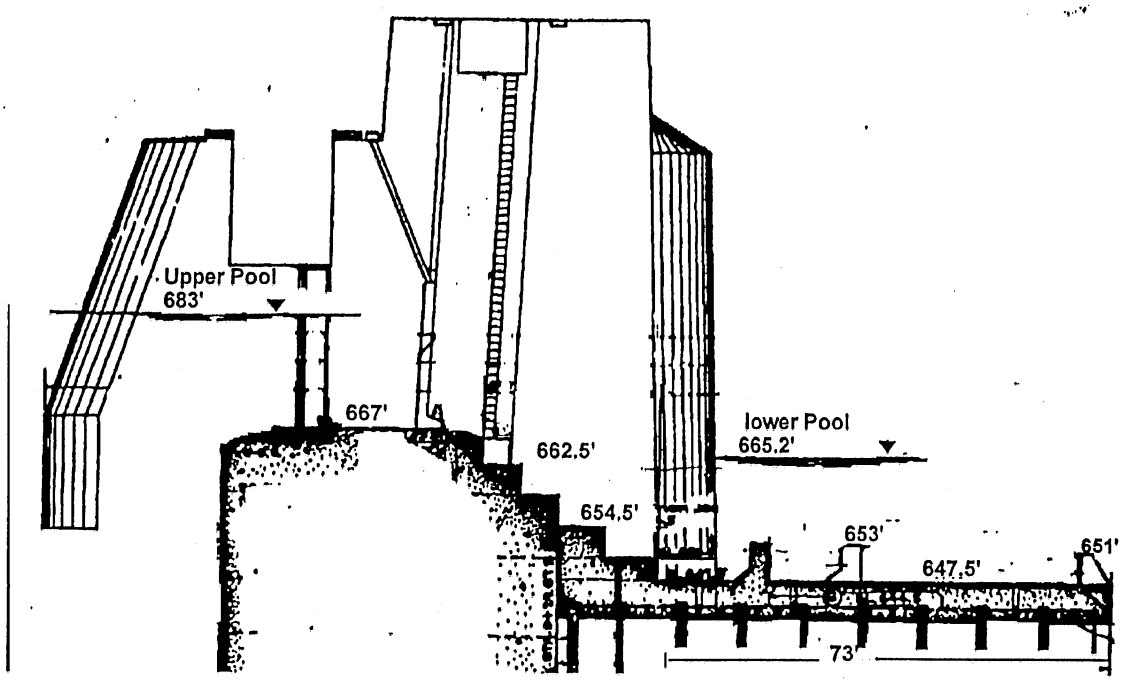

Cross section of lift gate at Montgomery Lock and Dam

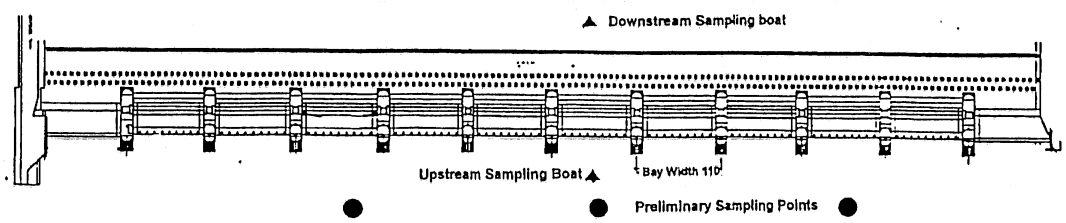

Planview and sampling points at Montgomery Lock and Dam

Figure 2

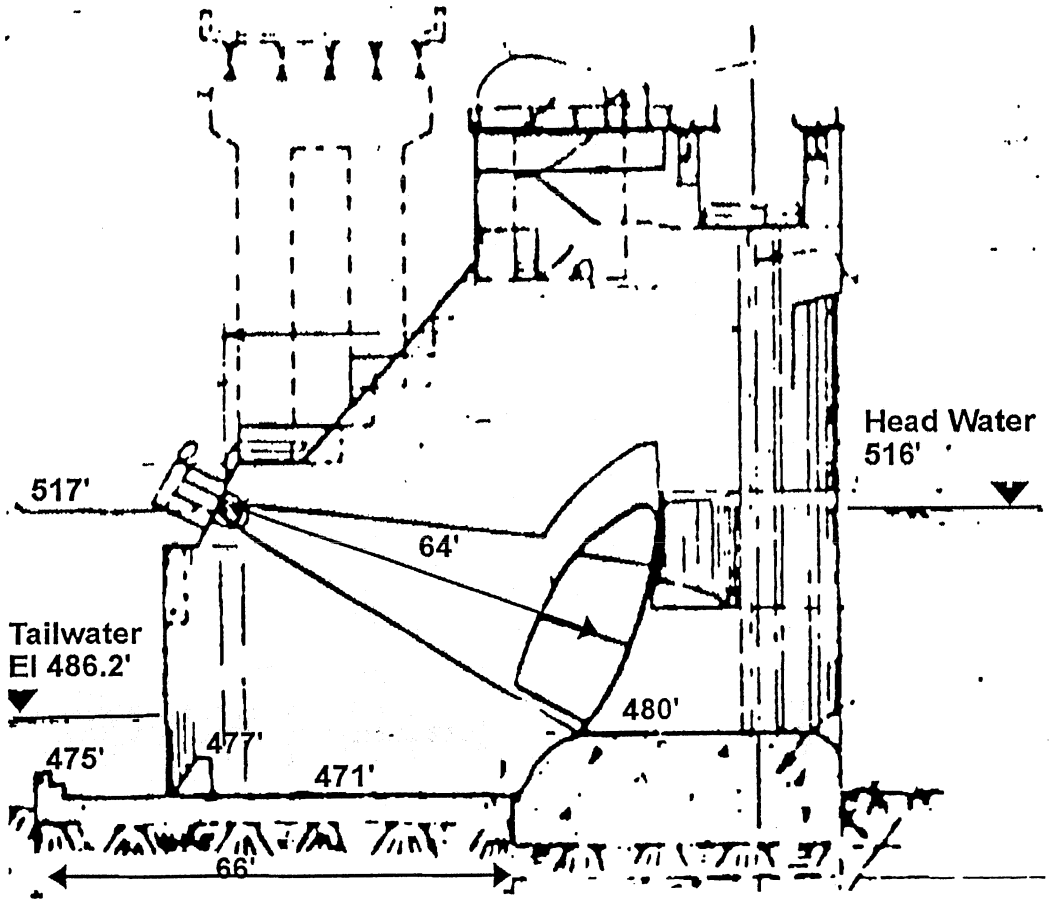

Cross Section across Tainter Gate at Greenup Lock and Dam

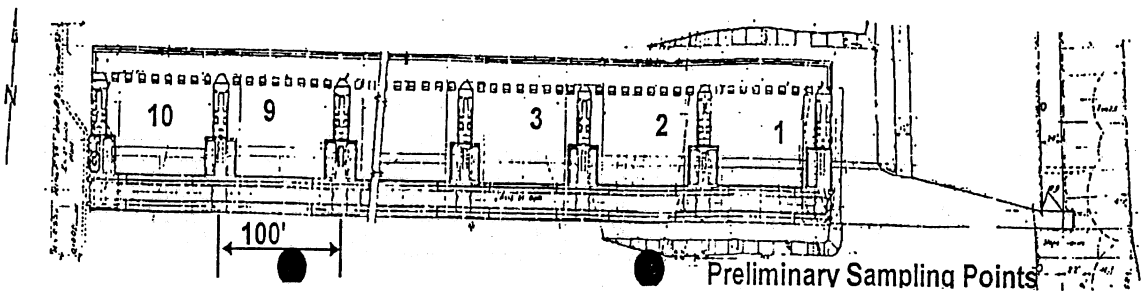

Planview of Greenup Lock and Dam

Figure 3

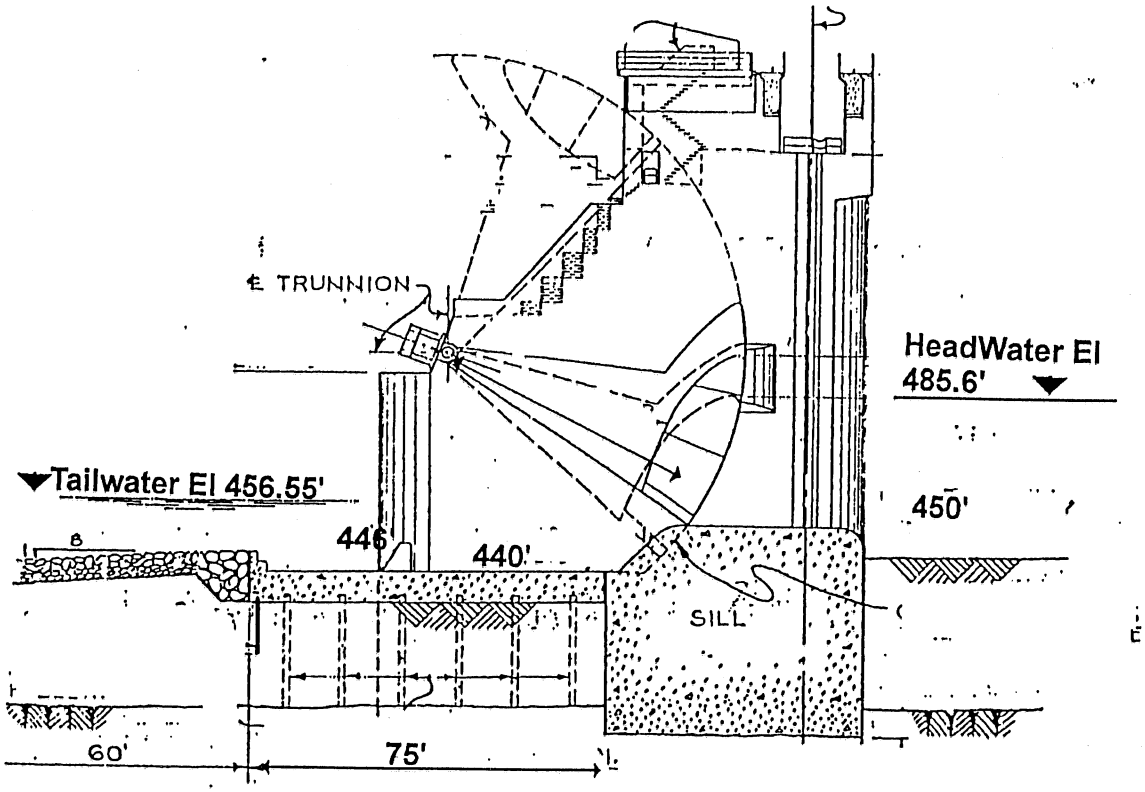

Cross Section across Meldhal Lock and Dam

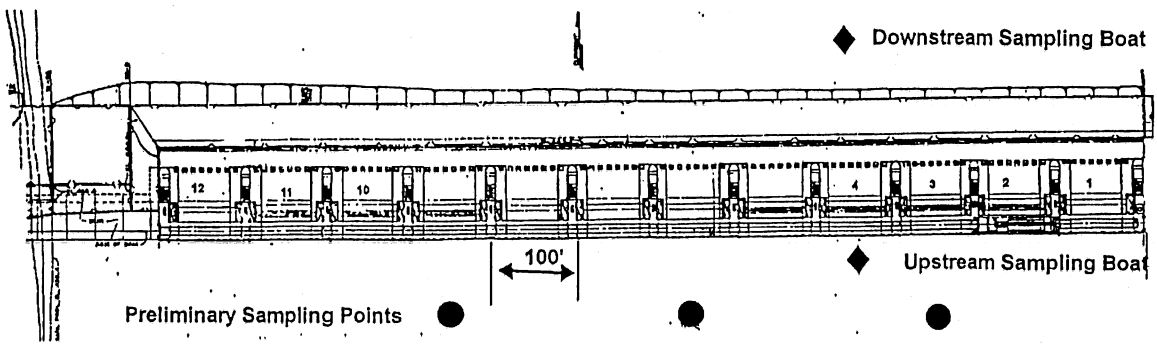

: Planview and sampling point at Meldhal Lock and Dam

Figure 4

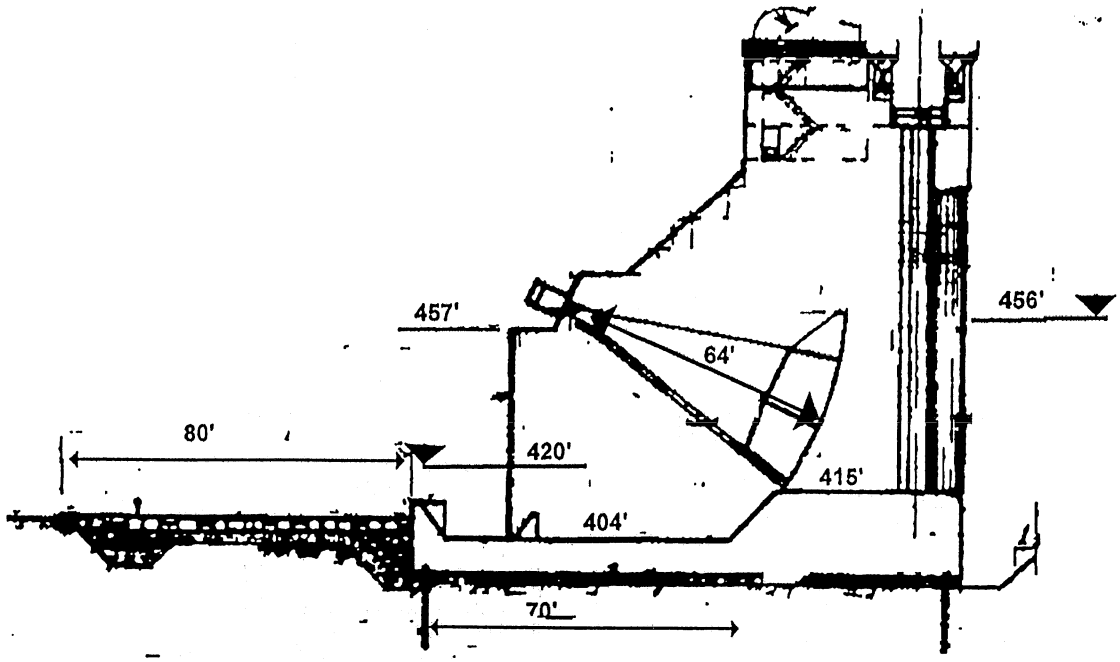

Cross Section across tainter gate at Markland Lock and Dam

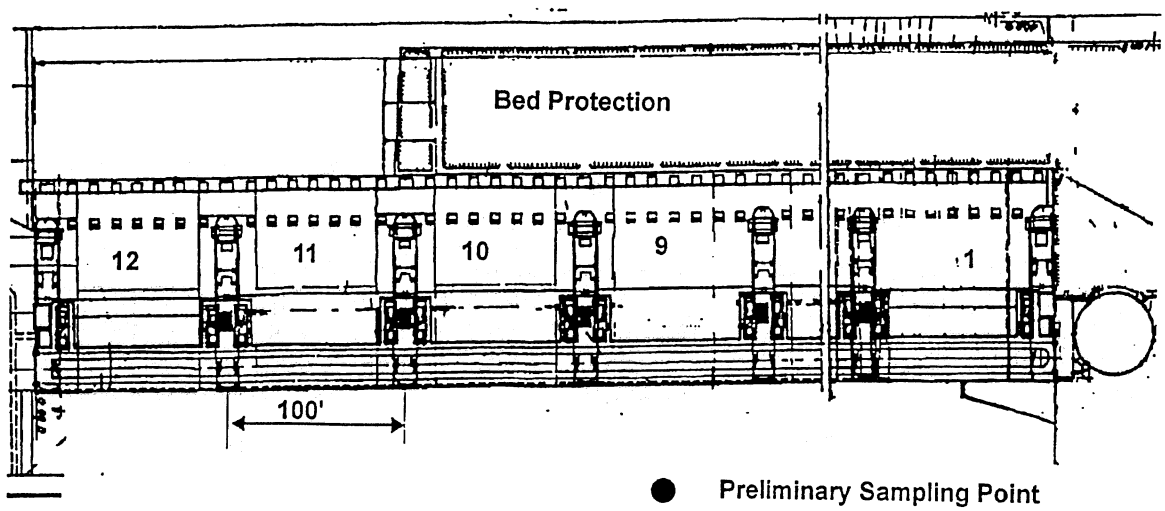

Planview and Sampling point at Markland Lock and Dam

Figure 5

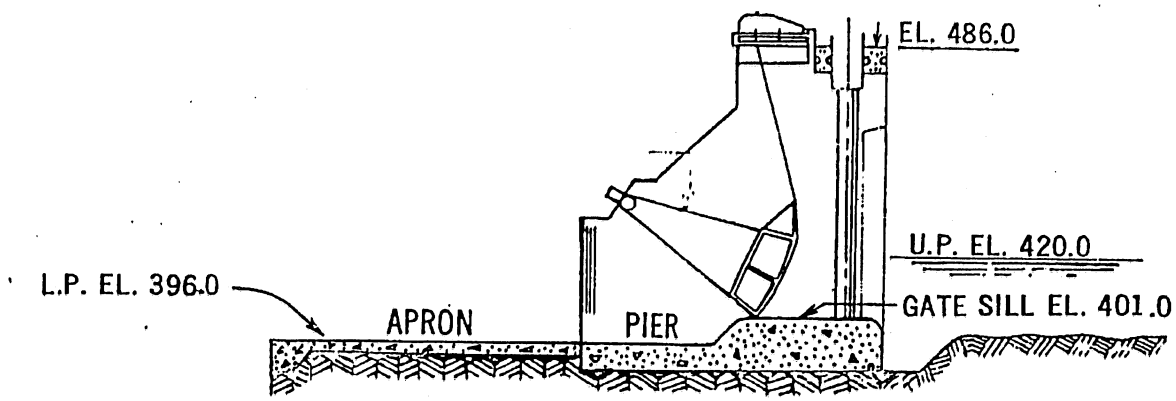

Cross Section across upper gates at McAlpine Lock and Dam

Figure 6

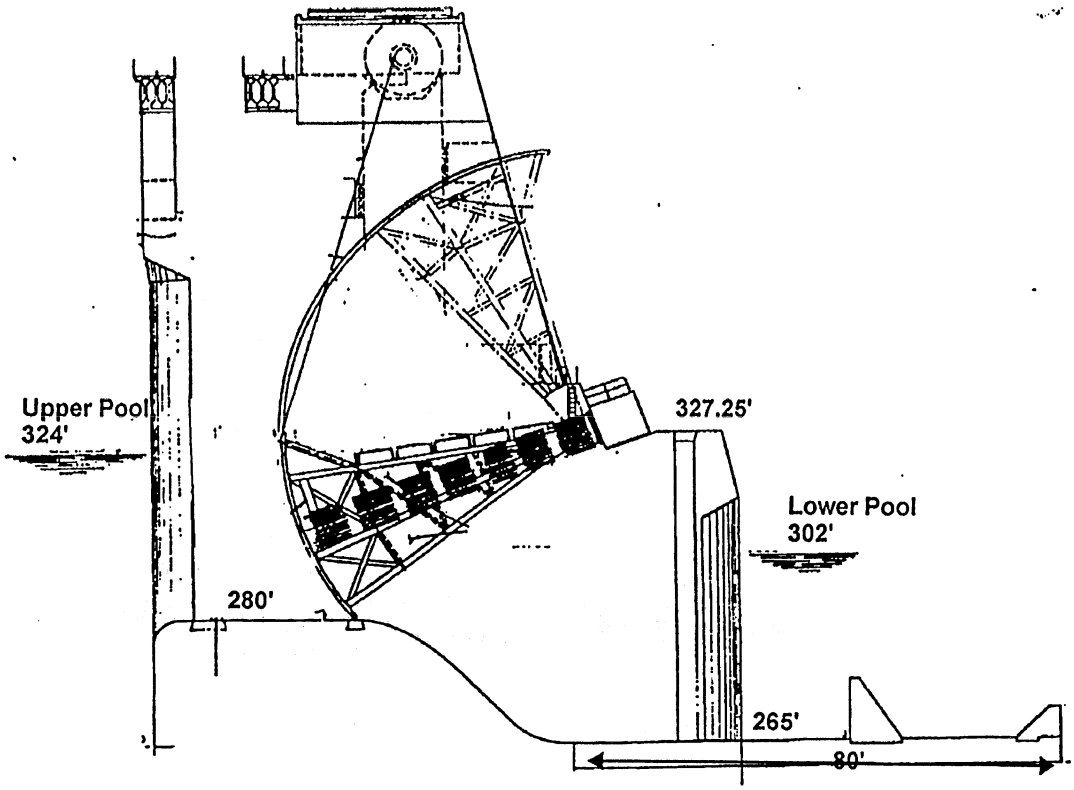

Cross section of tainter gate at Smithland Lock and Dam

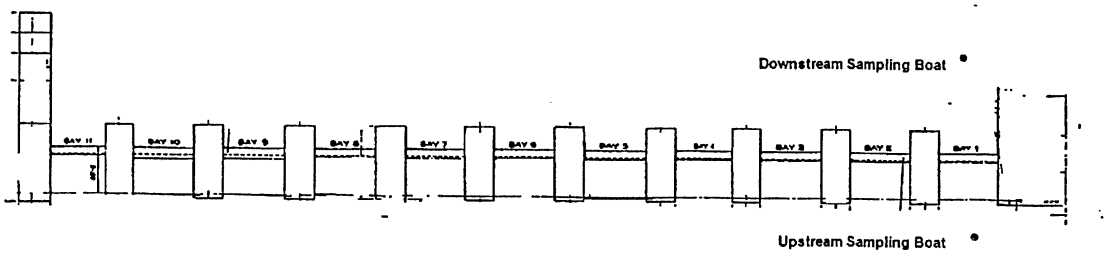

Planview at Smithland Lock and Dam

Figure 7

Appendix B

Methane Sampler

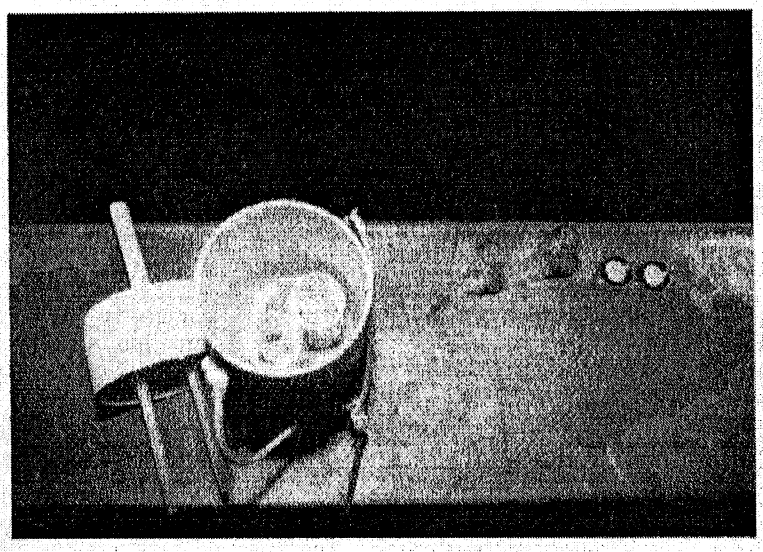

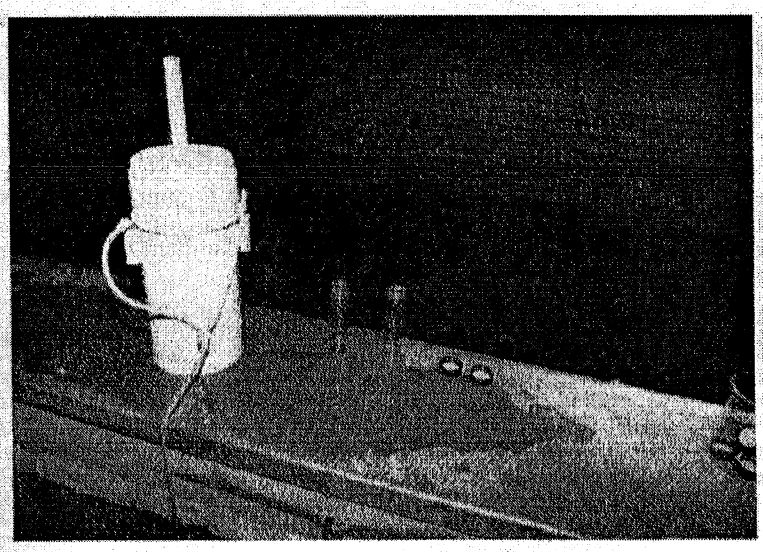

Appendix C

Analysed Methane Data

Greenup Lock and Dam & Hydropower

August 22 & 23, 1996

Methane Field Data and Transfer Efficiency Calculation

Preliminary Upstream Data

Response Factor	Bottle #	Time	Location (quarter pt.	Depth (feet)	[CH_4] (ug/L)	uncert. [CH_4]
1.92E-07	S-7c	1248	pre-25	30.0	3.44	0.187
1.92E-07	S-98c	1306	pre-50	40.0	3.15	0.074
1.92E-07	S-165c	1332	pre-75	40	3.56	0.245

[Gate Number]

Response Factor	Bottle #	Time	Location (up/down)	Gate (feet)	[CH_4] (ug/L)	uncert. [CH_4]	Transfer Efficiency	uncert. Transfer Efficiency
1.92E-07	S-153c	1435	down	0.5	3.31	0.16	-0.01	0.068
1.92E-07	S-24c	1440	up	0.5	3.28	0.15		
1.92E-07	731c	1512	down	1.0	3.15	0.10	0.04	0.046
1.92E-07	S-179c	1509	up	1	3.26	0.12		
1.92E-07	854c	1538	down	1.5	3.05	0.12	0.11	0.057
1.92E-07	S-104c	1539	up	1.5	3.43	0.17		
1.92E-07	552c	1606	down	2	2.89	0.17	0.15	0.078
2.00E-07	S-23c	1608	up	2	3.39	0.24		
2.00E-07	723c	1640	down	2.5	2.48	0.09	0.29	0.038
2.00E-07	S-105c	1634	up	2.5	3.49	0.14		
2.00E-07	301c	1708	down	3	2.23	0.08	0.33	0.038
2.00E-07	S-134c	1707	up	3	3.34	0.14		
2.00E-07	475c	1738	down	3.5	2.32	0.11	0.33	0.040
2.00E-07	S-131c	1735	up	3.5	3.48	0.13		
2.00E-07	471c	1806	down	4	2.48	0.16	0.26	0.056
2.00E-07	S-164c	1807	up	4	3.34	0.14		
2.00E-07	561c	1835	down	4.5	2.55	0.20	0.31	0.058
2.00E-07	S-124c	1836	up	4.5	3.73	0.12		
2.00E-07	597c	1905	down	5	2.17	0.21	0.38	0.067
2.00E-07	S-121c	1903	up	5	3.51	0.17		

Hydropower Data Collected on 8/23/96

Response Factor	Bottle #	Time	Location (up/down)	Gate (feet)	[CH_4] (ug/L)	uncert. [CH_4]	Transfer Efficiency	uncert. Transfer Efficiency
2.03E-07	773c	1616	down	10,10,10	4.36	0.2	0.00	0.081
2.03E-07	348c	1617	up	10,10,10	4.37	0.3		
2.03E-07	s-129c	1100	down	10,10,80	4.81	0.2	-0.04	0.077
2.03E-07	s-13c	1102	up	10,10,80	4.60	0.3		
2.03E-07	805c	1436	down	10,50,50	4.89	0.2	0.08	0.049
2.03E-07	s-136c	1433	up	10,50,50	5.32	0.1		
2.03E-07	533c	1141	down	10,80,10	3.65	0.1	0.04	0.053
2.03E-07	s-92c	1132	up	10,80,10	3.78	0.2		
2.03E-07	867c	1545	down	50,10,10	4.50	0.4	-0.02	0.108
2.03E-07	21c	1538	up	50,10,10	4.42	0.3		
2.03E-07	s-170c	1508	down	50,50,10	3.89	0.3	0.12	0.082
2.03E-07	s-34c	1507	up	50,50,10	4.40	0.2		
2.03E-07	s-158c	1351	down	50,50,50	4.34	0.1	0.29	0.095
2.03E-07	s-1c	1349	up	50,50,50	6.15	0.8		
2.03E-07	s-64c	1244	down	80,10,10	4.07	0.1	0.27	0.052
2.03E-07	s-5c	1245	up	80,10,10	5.57	0.3		
2.03E-07	s-2c	1213	down	80,80,10	3.99	0.2	0.24	0.046
2.03E-07	s-44c	1211	up	80,80,10	5.26	0.2		
2.03E-07	s-184c	1021	down	80,80,80	4.11	0.4	0.47	0.055
2.03E-07	s-35c	1020	up	80,80,80	7.76	0.4		

Markland Lock and Dam & Hydropower

August 31 & September 1, 1996

Methane Field Data and Transfer Efficiency Calculation

Preliminary Upstream Data

Response Factor	Bottle #	Time	Location (quarter pt.	Depth (feet)	$[CH_4]$ (ug/L)	uncert. $[CH_4]$
1.82E-07	s-5h	915	pre-25	50	7.45	0.25
1.82E-07	s-68h	931	pre-50	50	7.06	0.18
1.82E-07	s-48h	951	pre-75	35	17.10	0.53

[Gate Number]

Response Factor	Bottle #	Time	Location (up/down)	Gate (feet)	$[CH_4]$ (ug/L)	uncert. $[CH_4]$	Transfer Efficiency	uncert. Transfer Efficiency
1.82E-07	s-30h	1109	down	0.5	9.26	0.25	0.15	0.494
1.82E-07	s-6h	1111	up	0.5	10.91	6.33		
1.82E-07	776h	1139	down	1.0	8.81	0.17	0.16	0.510
1.82E-07	s-125h	1138	up	1.0	10.46	6.32		
1.82E-07	787h	1205	down	1.5	9.06	0.33	0.10	0.569
1.82E-07	s-28h	1203	up	1.5	10.04	6.32		
1.82E-07	348h	1232	down	2	9.20	0.22	0.07	0.589
1.82E-07	s-39h	1229	up	2	9.94	6.32		
1.82E-07	s-183h	1300	down	2.5	8.75	0.23	0.28	0.372
1.82E-07	s-22h	1258	up	2.5	12.23	6.35		
1.82E-07	s-128h	1331	down	3	9.07	0.23	0.26	0.387
1.82E-07	s-146h	1328	up	3	12.20	6.34		
1.82E-07	s-13ah	1402	down	3.5	9.91	0.50	0.32	0.295
1.82E-07	s-1h	1356	up	3.5	14.63	6.34		
1.90E-07	s-181h	1427	down	4	10.37	0.45	0.25	0.343
1.82E-07	s-16h	1427	up	4	13.89	6.35		
1.82E-07	s-95h	1455	down	4.5	9.74	0.25	0.03	0.609
1.82E-07	s-54h	1450	up	4.5	10.07	6.33		
1.90E-07	310h	1523	down	5	10.16	0.52	0.28	0.329
1.82E-07	s-42h	1521	up	5	14.02	6.33		

Hydropower Data

Response Factor	Bottle #	Time	Location (up/down)	Gate (feet)	$[CH_4]$ (ug/L)	uncert. $[CH_4]$	Transfer Efficiency	uncert. Transfer Efficiency
1.90E-07	877i	1037	down	100 all	14.08	0.90	0.18	1.387
1.90E-07	s-171i	1033	up	100 all	17.20	29.12		
1.90E-07	866i	1104	down	100,90,90	15.60	0.46	0.06	1.643
1.90E-07	s-55i	1105	up	100,90,90	16.63	29.11		
1.90E-07	s-87i	1354	down	70,70,80	22.15	3.87	0.30	0.665
1.90E-07	557i	1357	down	70,70,80	31.49	29.27		
1.90E-07	437i	1325	down	70,80,70	19.88	0.32	0.42	0.492
1.90E-07	s-53i	1320	up	70,80,70	34.32	29.11		
1.90E-07	190i	111	down	80,70,70	19.51	0.45	0.14	1.108
1.90E-07	s-18i	1205	up	80,70,70	22.65	29.12		
1.90E-07	727i	1133	down	90,100,90	17.65	0.25	0.01	1.609
1.90E-07	s-71i	1132	up	90,100,90	17.87	29.12		
1.90E-07	403i	1249	down	90,90,100	25.13	0.58	0.28	0.607
1.90E-07	s-184i	1245	up	90,90,100	34.74	29.15		

Meldahl Lock and Dam

August 24, 1996

Methane Field Data and Transfer Efficiency Calculation

Preliminary Upstream Data

Response Factor	Bottle #	Time	Location (quarter pt.	Depth (feet)	[CH_4] (ug/L)	uncert. [CH_4]
2.03E-07	s-38d	1058	pre-25	35.0	7.15	0.4
2.03E-07	s-160d	1034	pre-50	35.0	6.32	0.2
2.03E-07	s-4d	1015	pre-75	35.0	6.55	0.2

[Gate Number]

Response Factor	Bottle #	Time	Location (up/down)	Gate (feet)	[CH_4] (ug/L)	uncert. [CH_4]	Transfer Efficiency	uncert. Transfer Efficiency
2.11E-07	890d	1713	down	0.5	5.58	0.10	-0.03	0.199
2.16E-07	776d	1712	up	0.5	5.42	1.04		
2.11E-07	s-23d	1636	down	1	5.25	0.41	0.04	0.198
2.16E-07	385d	1641	up	1	5.48	1.05		
2.11E-07	s-45d	1601	down	1.5	6.17	0.45	-0.07	0.210
2.16E-07	389d	1602	up	1.5	5.74	1.04		
2.11E-07	s-27d	1536	down	2	4.53	0.24	0.19	0.161
2.16E-07	9d	1533	up	2	5.61	1.08		
2.11E-07	s-138d	1505	down	2.5	4.85	0.22	0.05	0.199
2.11E-07	s-41d	1504	up	2.5	5.11	1.04		
2.11E-07	s-188d	1433	down	3	5.79	0.24	-0.02	0.194
2.11E-07	349d	1433	up	3	5.67	1.06		
2.11E-07	376d	1349	down	3.5	4.64	0.30	0.13	0.177
2.03E-07	8d	1350	up	3.5	5.35	1.04		
2.11E-07	s-32d	1312	down	4	4.91	0.30	0.07	0.193
2.03E-07	472d	1314	up	4	5.30	1.05		
2.11E-07	s-143d	1243	down	4.5	4.83	0.26	0.19	0.148
2.11E-07	s-104d	1244	up	4.5	5.96	1.04		
2.11E-07	s-135d	1136	down	5	5.53	0.20	0.12	0.152
2.03E-07	s-67d	1134	up	5	6.29	1.07		

Montgomery Island Lock and Dam

August 19, 1996

Methane Field Data and Transfer Efficiency Calculation

Preliminary Upstream Data

Response Factor	Bottle #	Time	Location (quarter pt.	Depth (feet)	$[CH_4]$ (ug/L)	uncert. $[CH_4]$
1.63E-07	s-102a	1130	pre-25	30.0	4.65	0.1
1.63E-07	s-103a	1155	pre-50	26.0	5.23	0.1
1.63E-07	s-133a	1240	pre-75	25.0	6.23	0.2

[Gate Number]

Response Factor	Bottle #	Time	Location (up/down)	Gate (feet)	$[CH_4]$ (ug/L)	uncert. $[CH_4]$	Transfer Efficiency	uncert. Transfer Efficiency
1.63E-07	s-6a	1421	down	0.5	1.42	0.14	0.68	0.071
1.63E-07	s-144a	1426	up	0.5	4.47	0.91		
1.63E-07	s-37a	1520	down	1	1.53	0.11	0.68	0.066
1.63E-07	s-107a	1512	up	1	4.76	0.91		
1.63E-07	s-46a	1554	down	1.5	1.50	0.10	0.73	0.050
1.99E-07	s-108a	1559	up	1.5	5.44	0.91		
1.63E-07	s-9a	1636	down	2	1.74	0.18	0.68	0.063
1.99E-07	s-153a	1631	up	2	5.44	0.91		
1.63E-07	s-73a	1718	down	2.5	2.04	0.10	0.64	0.060
1.99E-07	s-162a	1714	up	2.5	5.70	0.92		
1.99E-07	s-29a	1748	down	3	3.14	0.16	0.53	0.068
2.08E-07	s-171a	1750	up	3	6.74	0.93		
1.99E-07	s-15a	1823	down	3.5	2.64	0.23	0.57	0.074
2.08E-07	s-182a	1827	up	3.5	6.17	0.91		
1.99E-07	s-56a	1905	down	4	3.26	0.23	0.54	0.085
2.08E-07	s-119a	1903	up	4	7.05	1.19		
1.99E-07	s-13a	1951	down	4.5	3.60	0.31	0.44	0.094
2.08E-07	s-128a	1951	up	4.5	6.41	0.92		
1.99E-07	s-25a	1927	down	spillway	3.02	0.20	0.58	0.031
2.08E-07	s-125a	1930	up	spillway	7.12	0.23		

McAlpine Lock and Dam

August 26 & 27, 1996

Methane Field Data and Transfer Efficiency Calculation

Preliminary Upstream Data Collected on 8/26/96

Response Factor	Bottle #	Time	Location (quarter pt.	Depth (feet)	$[CH_4]$ (ug/L)	uncert. $[CH_4]$
1.85E-07	s-24e	941	pre-25	25.0	6.69	0.2
1.85E-07	s-63e	921	pre-50	25	6.71	0.4
1.85E-07	86e	855	pre-75	23	8.29	0.2

Test Gate #3 and Hydropower Data Collected on 8/26/96

2.87274

Response Factor	Bottle #	Time	Location (up/down)	Gate (feet)	$[CH_4]$ (ug/L)	uncert. $[CH_4]$	Transfer Efficiency	uncert. Transfer Efficiency
1.85E-07	749e	1006	down	0.5	0.46	0.08	0.93	0.025
1.85E-07	s-52e	1005	up	0.5	6.18	1.71		
1.85E-07	351e	1038	down	1	1.69	0.33	0.73	0.096
1.85E-07	s-19e	1045	up	1	6.19	1.83		
1.85E-07	s-17e	1112	down	1.5	1.86	0.10	0.54	0.199
1.85E-07	603e	1119	up	1.5	4.00	1.70		
1.85E-07	s-102e	1205	down	2	2.37	0.17	0.42	0.247
2.03E-07	370e	1210	up	2	4.06	1.70		
1.85E-07	s-100e	1239	down	2.5	2.72	0.15	0.28	0.331
1.85E-07	s-82e	1240	up	2.5	3.75	1.70		
1.85E-07	561e	1311	down	3	4.16	0.44	0.12	0.335
2.03E-07	s-140e	1218	up	3	4.70	1.71		
1.85E-07	452e	1355	down	3.5	2.55	0.18	0.58	0.120
2.03E-07	s-31e	1348	up	3.5	6.15	1.71		
1.85E-07	558e	1426	down	4	1.98	0.10	0.70	0.080
1.85E-07	s-25e	1426	up	4	6.58	1.71		
1.85E-07	233e	1456	down	4.5	1.93	0.14	0.73	0.066
1.85E-07	s-117e	1455	up	4.5	7.28	1.72		
1.85E-07	s-125e	1550	down	5	2.00	0.11	0.73	0.063
1.85E-07	718e	1547	up	5	7.51	1.73		
1.85E-07	s-88e	1338	down	hydro	6.98	0.32	0.26	0.147
2.03E-07	s-67e	1334	up	hydro	9.40	1.81		

Preliminary Upstream Data Collected on 8/27/96

Response Factor	Bottle #	Time	Location (quarter pt.	Depth (feet)	$[CH_4]$ (ug/L)	uncert. $[CH_4]$
2.03E-07	s-46f	1153	pre-25	15	11.52	0.91
2.03E-07	s-65f	1220	pre-50	15.0	11.29	1.15
2.03E-07	s-76f	1240	pre-75	15.0	13.01	0.59

Test Gate #8 Data Collected on 8/27/96

Response Factor	Bottle #	Time	Location (up/down)	Gate (feet)	$[CH_4]$ (ug/L)	uncert. $[CH_4]$	Transfer Efficiency	uncert. Transfer Efficiency
2.03E-07	s-188f	1505	down	1	4.78	0.17	0.41	0.032
2.03E-07	188f	1434	down	2	4.92	0.23	0.36	0.038
2.03E-07	s-35f	1439	up	2	7.69	0.28		
2.03E-07	s-93f	1404	down	3	6.07	0.17	0.22	0.060
2.03E-07	21f	1400	up	3	7.75	0.55		
2.03E-07	s-12f	1330	down	4	7.89	0.31	0.09	0.057
2.03E-07	s-174f	1330	up	4	8.68	0.42		

Smithland Lock and Dam

August 29, 1996

Methane Field Data and Transfer Efficiency Calculation

Preliminary Upstream Data

Response Factor	Bottle #	Time	Location (quarter pt.	Depth (feet)	[CH_4] (ug/L)	uncert. [CH_4]
1.96E-07	s-77g	1135	pre-25	14.0	9.74	0.5
1.96E-07	s-109g	1013	pre-50	35.0	7.55	0.1
1.96E-07	s-8g	954	pre-75	35.0	6.72	0.2

[Gate Number]

Response Factor	Bottle #	Time	Location (up/down)	Gate (feet)	[CH_4] (ug/L)	uncert. [CH_4]	Transfer Efficiency	uncert. Transfer Efficiency
1.96E-07	s-28g	1138	down	0.5	5.83	0.2	0.07	0.174
1.96E-07	s-145g	1130	up	0.5	6.26	1.1		
1.96E-07	s-81g	1206	down	1	6.12	0.1	0.01	0.179
1.96E-07	s-100g	1210	up	1	6.18	1.1		
1.96E-07	s-24g	1238	down	1.5	6.22	0.3	0.07	0.160
1.96E-07	s-99g	1234	up	1.5	6.68	1.1		
1.96E-07	s-165g	1357	down	2	6.42	0.2	0.15	0.137
1.96E-07	s-62g	1352	up	2	7.58	1.2		
1.96E-07	s-149g	1423	down	2.5	6.45	0.2	0.01	0.174
1.96E-07	81g	1420	up	2.5	6.51	1.1		
1.96E-07	s-115g	1457	down	3	6.26	0.2	0.01	0.175
1.96E-07	s-51g	1456	up	3	6.34	1.1		
1.96E-07	s-187g	1521	down	3.5	6.39	0.2	0.03	0.168
1.96E-07	82g	1521	up	3.5	6.56	1.1		
1.96E-07	844g	1553	down	4	5.71	0.3	0.08	0.170
1.82E-07	s-43g	1551	up	4	6.22	1.1		
1.82E-07	597g	1623	down	4.5	6.00	0.2	0.08	0.163
1.82E-07	s-2g	1618	up	4.5	6.49	1.1		
1.82E-07	s-167g	1648	down	5	5.63	0.4	0.03	0.196
1.82E-07	67g	1646	up	5	5.79	1.1		

Belleville Lock and Dam

September 12 & 13, 1995

Methane Field Data and Transfer Efficiency Calculation

Response Factor	Bottle #	Time	Location (up/down)	Gate (feet)	Mean CH_4 water (ug/L)	Uncertainity Mean CH_4 water	CH_4 Transfer Efficiency	Uncertainity CH_4 Trans. Eff.
2.73E-07	432	14:20	down	0	7.84	0.17	-0.49	0.041
2.73E-07	277	14:05	up	0	5.27	0.09		
2.73E-07	413	12:22	down	2	7.37	0.29	-0.45	0.070
2.73E-07	272	12:15	up	2	5.08	0.14		
2.73E-07	409	12:57	down	3	6.87	0.41	-0.39	0.135
2.73E-07	217	12:47	up	3	4.96	0.38		
2.73E-07	452	13:18	down	4	6.54	0.20	-0.21	0.044
2.73E-07	293	13:16	up	4	5.43	0.10		
2.73E-07	434	13:30	down	5	5.28	0.15	0.04	0.048
2.73E-07	227	13:30	up	5	5.49	0.22		

Gate #3 Data collected on 9/13/95

Response Factor	Bottle #	Time	Location (up/down)	Gate (feet)	Mean CH_4 water (ug/L)	Uncertainity Mean CH_4 water	CH_4 Transfer Efficiency	Uncertainity CH_4 Trans. Eff.
2.73E-07	414	14:53	down	1	7.85	0.20	-0.61	0.163
2.73E-07	339	14:45	up	1	4.87	0.48		
2.73E-07	418	14:28	down	1.5	7.87	0.13	-0.29	0.047
2.73E-07	313	14:25	up	1.5	6.08	0.20		
2.73E-07	428	14:07	down	2	7.17	0.35	-0.42	0.110
2.73E-07	334	14:01	up	2	5.07	0.30		
2.73E-07	421	12:39	down	2.5	7.76	0.25	-0.40	0.050
2.73E-07	269	12:33	up	2.5	5.53	0.08		
2.73E-07	433	12:10	down	3	7.35	0.11	-0.20	0.040
2.73E-07	246	12:04	up	3	6.14	0.18		
2.73E-07	451	10:45	down	3.5	7.03	0.17	-0.27	0.047
2.73E-07	256	10:32	up	3.5	5.55	0.16		
2.73E-07	371	11:41	down	4	6.39	0.22	-0.14	0.063
2.73E-07	338	11:35	up	4	5.58	0.24		
2.73E-07	455	13:05	down	4.5	7.50	0.18	-0.25	0.049
2.73E-07	261	13:00	up	4.5	6.02	0.18		
2.73E-07	396	11:18	down	5	6.55	0.11	-0.14	0.032
2.73E-07	209	11:13	up	5	5.74	0.13		

Racine Hydropower

September 15, 1995

Methane Field Data and Transfer Efficiency Calculation

Gate Data

Response Factor	Bottle #	Time	Location (up/down)	G. O. (%)	Mean $CH_{4\ water}$ (ug/L)	Uncertainity Mean $CH_{4\ water}$	CH_4 Transfer Efficiency	Uncertainity CH_4 Trans. Eff.
2.73E-07	337	10:48	down	35	9.76	0.29	0.21	0.0247
2.73E-07	720	10:44	up	35	12.35	0.14		
2.73E-07	295	11:51	down	45	9.43	0.10	0.19	0.0166
2.73E-07	749	11:53	up	45	11.70	0.21		
2.73E-07	315	12:44	down	55	9.95	0.26	0.17	0.0238
2.73E-07	744	11:14	up	55	11.94	0.13		
2.73E-07	301	13:36	down	70	9.88	0.30	0.12	0.0286
2.73E-07	756	13:33	up	70	11.16	0.12		
2.73E-07	359	14:54	down	91	10.23	0.25	0.14	0.0226
2.73E-07	764	14:26	up	91	11.92	0.13		

Racine Lock and Dam

October 4, 1995

Methane Field Data and Transfer Efficiency Calculation

Gate #5 Data

Response Factor	Bottle #	Time	Location (up/down)	Gate (feet)	Mean $CH_{4\ water}$ (ug/L)	Uncertainity Mean $CH_{4\ water}$	CH_4 Transfer Efficiency	Uncertainity CH_4 Trans. Eff.
2.73E-07	1385	14:51	down	0.5	6.41	0.07	-0.26	0.0376
2.73E-07	1383	15:00	up	0.5	5.09	0.14		
2.73E-07	1353	14:25	down	1	5.86	0.13	-0.19	0.0538
2.73E-07	1050	14:30	up	1	4.92	0.19		
2.73E-07	1377	14:03	down	1.5	4.80	0.26	0.29	0.0443
2.73E-07	1401	14:00	up	1.5	6.76	0.22		
2.73E-07	1114	13:27	down	2	8.43	0.27	-1.15	0.0862
2.73E-07	1357	13:30	up	2	3.91	0.10		
2.73E-07	1344	13:02	down	2.5	7.54	0.47	-0.48	0.1051
2.73E-07	1298	13:00	up	2.5	5.11	0.18		
2.73E-07	1293	12:40	down	3	7.09	0.10	-0.39	0.1011
2.73E-07	1343	12:45	up	3	5.11	0.37		
2.73E-07	1036	12:12	down	3.5	4.56	0.03	0.12	0.0115
2.73E-07	1359	12:15	up	3.5	5.19	0.06		
2.73E-07	1016	11:44	down	4	7.93	0.22	-0.27	0.0413
2.73E-07	1390	11:45	up	4	6.25	0.11		
2.73E-07	1368	11:22	down	4.5	7.01	0.33	-0.90	0.0954
2.73E-07	1045	11:15	up	4.5	3.69	0.07		
2.73E-07	1415	11:00	down	5	8.70	0.23	-1.13	0.0641
2.73E-07	1374	11:00	up	5	4.10	0.06		

RC Byrd Lock and Dam

October 6, 1995

Methane Field Data and Transfer Efficiency Calculation

[Gate Number]

Response Factor	Bottle #	Time	Location (up/down)	Gate (feet)	mean AC	deviation AC	uncert. AC	$[CH_4]$ (ug/L)	uncert. $[CH_4]$	Transfer Efficiency	uncert. Transfer Efficiency
2.73E-07	1313	13:37	down	0.5	10384	657	470	4.20	0.2	-0.04	0.215
2.73E-07	1408	13:40	up	0.5	10232	2886	2064	4.03	0.8		
2.73E-07	1139	12:59	down	1.5	15738	121	150	5.52	0.1	-0.06	0.149
2.73E-07	1144	13:00	up	1.5	12698	2487	1779	5.22	0.7		
2.73E-07	1233	12:39	down	2	13920	4580	3276	5.11	1.2	-0.35	0.591
2.73E-07	1345	12:44	up	2	9943	5156	3688	3.80	1.4	-	
2.73E-07	1081	12:17	down	2.5	6627	909	651	2.82	0.3	0.10	0.093
2.73E-07	1065	12:20	up	2.5	7683	345	247	3.14	0.1		
2.73E-07	1128	11:57	down	3	10212	339	242	3.84	0.1	0.43	0.020
2.73E-07	1395	11:58	up	3	16085	562	402	6.78	0.2		
2.73E-07	1307	11:33	down	3.5	8550	1600	1145	3.74	0.5	0.08	0.330
2.73E-07	1396	11:33	up	3.5	10148	4743	3393	4.08	1.4		
2.73E-07	1180	11:04	down	4	9813	2230	1595	3.83	0.6	0.12	0.330
2.73E-07	1095	11:08	up	4	10531	4964	3551	4.33	1.5		
2.73E-07	1278	10:40	down	4.5	8966	1339	958	3.63	0.4	0.37	0.080
2.73E-07	1242	10:40	up	4.5	13714	1310	937	5.74	0.4		
2.73E-07	1188	10:08	down	5	8140	564	403	3.33	0.2	0.43	0.030
2.73E-07	1279	10:20	up	5	14086	331	237	5.83	0.1		

Winfield Hydropower

October 12, 1995

Methane Field Data and Transfer Efficiency Calculation

Gate Data

Response Factor	Bottle #	Time	Location (up/down)	Gate %	Mean $CH_{4\ water}$ (ug/L)	Uncertainity Mean $CH_{4\ water}$	CH_4 Transfer Efficiency	Uncertainity CH_4 Trans. Eff.
2.73E-07	1350	12:11	down	35	9.52	0.19	0.36	0.014
2.73E-07	1230	12:15	up	35	14.84	0.11		
2.73E-07	1040	13:23	down	45	9.83	0.58	-0.02	0.060
2.73E-07	1054	13:20	up	45	9.64	0.06		
2.73E-07	1077	14:06	down	55	11.28	0.67	0.25	0.045
2.73E-07	1288	14:05	up	55	14.99	0.08		
2.73E-07	1362	14:50	down	70	16.00	0.03	-0.24	0.010
2.73E-07	1268	14:44	up	70	12.89	0.10		
2.73E-07	1392	15:02	down	75	11.99	0.04	0.13	0.040
2.73E-07	1068	13:29	up	75	13.82	0.63		

Appendix D

Analysed Oxygen Data

Greenup Lock and Dam
8/22/96

Dissolved Oxygen Data

Gate Setting	Location (up/down)	Sample Depth (feet)	Temperature (°C)	Percent Saturation	mean % saturation	Uncertainity % saturation
0.5	down	0.5	25.66	97.5	97.67	0.38
0.5	down	10	25.66	97.8		
0.5	down	18	25.66	97.7		
0.5	up	1	27.09	106.1	97.63	18.21
0.5	up	22	25.64	93.3		
0.5	up	38.7	25.66	93.5		
1	down	0.5	25.85	100.1	100.03	0.29
1	down	10.4	25.83	100.1		
1	down	18	25.83	99.9		
1	up	1	27.59	107.8	98.70	19.57
1	up	20.1	25.66	94		
1	up	41.4	25.68	94.3		
1.5	down	0.5	25.77	101.2	102.53	4.70
1.5	down	8.7	25.83	101.7		
1.5	down	16.1	25.83	104.7		
1.5	up	0.9	27.44	109.1	99.37	20.93
1.5	up	21.9	25.69	94.4		
1.5	up	39.7	25.75	94.6		
2	down	0.5	25.92	102.6	103.13	2.08
2	down	10.3	25.92	104.1		
2	down	15.2	25.94	102.7		
2	up	0.2	28.26	120.6	102.90	38.25
2	up	21.6	25.69	95.6		
2	up	40.7	25.68	92.5		
2.5	down	0.5	25.99	108.4	106.17	5.86
2.5	down	10.4	25.97	106.4		
2.5	down	15	25.97	103.7		
2.5	up	0.5	27.9	123.2	104.13	41.16
2.5	up	21.6	25.71	96.1		
2.5	up	39.4	25.65	93.1		
3	down	0.5	25.97	109.4	109.30	2.86
3	down	10.1	25.89	108.1		
3	down	12.7	25.91	110.4		
3	up	0.8	27.37	117.7	101.73	34.47
3	up	21.1	25.68	95		
3	up	39.8	25.66	92.5		
3.5	down	0.5	25.86	108	109.33	2.87
3.5	down	9.7	25.87	110		
3.5	down	15.2	25.91	110		
3.5	up	0.8	28.13	131.2	105.83	54.55
3.5	up	21.1	25.68	93.6		
3.5	up	40.6	25.64	92.7		
4	down	0.5	25.78	105.2	104.73	1.60
4	down	10.3	25.8	104		
4	down	15.6	25.8	105		
4	up	0.1	27.53	129.3	106.20	49.93
4	up	21.5	25.77	96.7		
4	up	39.4	25.66	92.6		
4.5	down	0.5	25.73	102.8	103.10	1.74
4.5	down	9.3	25.71	103.9		
4.5	down	15.9	25.73	102.6		
4.5	up	0.4	27.04	116.5	101.70	31.82
4.5	up	21.6	25.72	94.3		
4.5	up	40.7	25.66	94.3		
5	down	0.5	25.71	106	106.33	1.43
5	down	9.9	25.73	106		
5	down	16.4	25.71	107		
5	up	0.9	26.52	115	101.57	29.24
5	up	21.4	25.9	96.7		
5	up	39.5	25.68	93		

Greenup Hydropower
8/23/96

Dissolved Oxygen Data

Gate Setting %	Location (up/down)	Sample Depth (feet)	Temperature (°C)	Percent Saturation	mean % saturation	Uncertainity % saturation
10,10,10	down	0.5	25.82	103.1	102.93	0.38
10,10,10	down	9.9	25.82	102.9		
10,10,10	down	16.8	25.89	102.8		
10,10,10	up	0.4	27.25	117	99.53	37.56
10,10,10	up	19.7	25.94	90.5		
10,10,10	up	29.6	25.91	91.1		
50,10,10	down	0.5	25.91	103.8	107.00	7.23
50,10,10	down	8.5	25.86	107.7		
50,10,10	down	13.1	25.89	109.5		
50,10,10	up	0.3	28.24	118.9	100.27	40.06
50,10,10	up	20.1	25.92	90.8		
50,10,10	up	24.5	25.93	91.1		
50,50,10	down	0.5	25.89	102.8	102.43	0.87
50,50,10	down	9	26.01	102.4		
50,50,10	down	11.4	25.97	102.1		
50,50,10	up	0.9	27.94	115.9	99.17	35.98
50,50,10	up	19.8	25.89	90.6		
50,50,10	up	22.7	25.89	91		
10,50,50	down	0.5	25.82	99.2	100.13	2.82
10,50,50	down	10.4	25.82	99.8		
10,50,50	down	15.9	25.91	101.4		
10,50,50	up	0.3	27.27	119	100.37	40.08
10,50,50	up	19.4	25.95	90.6		
10,50,50	up	29.8	25.97	91.5		
50,50,50	down	0.5	25.71	100.1	101.57	3.31
50,50,50	down	10	25.78	101.9		
50,50,50	down	14.1	25.8	102.7		
50,50,50	up	0.4	27.58	114	98.87	32.55
50,50,50	up	17.1	25.89	91		
50,50,50	up	29.5	25.91	91.6		
80,10,10	down	0.5	25.76	99.6	100.47	1.88
80,10,10	down	9	25.78	101		
80,10,10	down	17	25.74	100.8		
80,10,10	up	0.5	26.48	100.5	92.80	16.59
80,10,10	up	20.2	25.87	88.5		
80,10,10	up	29.8	25.89	89.4		
80,80,10	down	0.5	25.73	115.3	107.90	16.14
80,80,10	down	8	25.71	103.1		
80,80,10	down	11.4	25.73	105.3		
80,80,10	up	0.5	26.77	99.4	92.63	14.64
80,80,10	up	20.3	25.83	89.9		
80,80,10	up	31.4	25.83	88.6		
10,80,10	down	0.5	25.67	101.5	103.10	7.31
10,80,10	down	9.4	25.67	101.3		
10,80,10	down	12	25.67	106.5		
10,80,10	up	0.5	26.48	101.2	94.43	14.55
10,80,10	up	18.5	25.79	90.9		
10,80,10	up	31.4	25.79	91.2		
10,10,80	down	0.5	25.65	97.1	97.33	0.52
10,10,80	down	10	25.67	97.5		
10,10,80	down	12	25.67	97.4		
10,10,80	up	0.9	26.3	98.7	93.93	10.26
10,10,80	up	19.7	25.79	91.7		
10,10,80	up	26.4	25.75	91.4		
80,80,80	down	0.5	25.63	98	113.77	35.97
80,80,80	down	8.3	25.63	126.5		
80,80,80	down	15.2	25.62	116.8		
80,80,80	up	0.8	25.96	96.3	93.60	5.96
80,80,80	up	12.3	25.73	91.7		
80,80,80	up	17	25.75	92.8		

Markland Lock and Dam
8/31/96

Dissolved Oxygen Data

Gate Setting	Location (up/down)	Sample Depth (feet)	Temperature (°C)	Percent Saturation	mean % saturation	Efficiency	Uncertainity in Efficiency
0.5	down	0.5	27.1	82.7	82.63	0.27	0.083
0.5	down	11.5	27.1	83.2			
0.5	down	21.2	27.1	82			
0.5	up	0.3	27.36	76.9	76.07		
0.5	up	30.1	27.1	75.7			
0.5	up	48.1	27.09	75.6			
1	down	0.5	27.1	87.5	86.33	0.43	0.156
1	down	14	27.1	86.8			
1	down	21	27.1	84.7			
1	up	0.4	27.4	76.7	75.87		
1	up	30.6	27.11	75.2			
1	up	48.2	27.1	75.7			
1.5	down	0.5	27.1	89.3	89.03	0.53	0.074
1.5	down	9.5	27.12	88.7			
1.5	down	14.4	27.1	89.1			
1.5	up	0.1	27.55	78.2	76.70		
1.5	up	30	27.11	76.2			
1.5	up	49	27.11	75.7			
2	down	0.5	27.1	96.4	93.43	0.72	0.353
2	down	9	27.1	94.1			
2	down	25	27.1	89.8			
2	up	0.4	27.51	78.2	76.23		
2	up	30.6	27.11	75.3			
2	up	47.9	27.09	75.2			
2.5	down	0.5	27.12	96.3	95.33	0.80	0.155
2.5	down	9.3	27.12	96			
2.5	down	16	27.12	93.7			
2.5	up	0.3	27.62	78.5	76.50		
2.5	up	30.2	27.13	75.4			
2.5	up	47.6	27.09	75.6			
3	down	0.5	27.13	96	96.47	0.85	0.067
3	down	8.9	27.12	97			
3	down	18	27.12	96.4			
3	up	0.3	27.64	79	75.77		
3	up	30.6	27.1	74.6			
3	up	47.5	27.09	73.7			
3.5	down	0.5	27.13	97.8	96.83	0.87	0.098
3.5	down	9.3	27.13	96.2			
3.5	down	17	27.13	96.5			
3.5	up	0.1	27.76	79.7	76.27		
3.5	up	30.1	27.17	74.7			
3.5	up	47.2	27.1	74.4			
4	down	0.5	27.13	97.7	97.67	0.90	0.054
4	down	10	27.13	98			
4	down	22.2	27.15	97.3			
4	up	0.3	27.88	81	76.77		
4	up	30.4	27.15	74.6			
4	up	48.5	27.11	74.7			
4.5	down	0.5	27.17	97.2	97.47	0.89	0.039
4.5	down	8	27.17	97.7			
4.5	down	14.6	27.17	97.5			
4.5	up	0.2	27.86	79.3	76.43		
4.5	up	30.5	27.15	75.5			
4.5	up	48.6	27.13	74.5			
5	down	0.5	27.17	98	97.90	0.91	0.027
5	down	6	27.17	97.9			
5	down	10.5	27.17	97.8			
5	up	0.3	28.13	79.7	76.93		
5	up	30.4	27.17	76.2			
5	up	48.7	27.13	74.9			

Markland Hydropower
9/1/96

Dissolved Oxygen Data

Gate Setting %	Location (up/down)	Sample Depth (feet)	Temperature (°C)	Percent Saturation	mean % saturation	Efficiency	Uncertainity in Efficiency
100 all	down	0.5	26.89	79.2	79.25	-0.01	0.080
100 all	down						
100 all	down	10.3	26.89	79.3			
100 all	up	0.4	27.04	80.1	79.40		
100 all	up	15.1	27	79			
100 all	up	25.3	27	79.1			
90,100,90	down	0.5	26.91	79.6	79.55	-0.01	0.129
90,100,90	down						
90,100,90	down	10	26.89	79.5			
90,100,90	up	0.4	27.13	80.9	79.73		
90,100,90	up	15.2	26.98	79.1			
90,100,90	up	25.7	26.96	79.2			
80,70,70	down	0.5	26.89	79.3	79.27	-0.02	0.216
80,70,70	down	8.7	26.89	79.3			
80,70,70	down	17.6	26.89	79.2			
80,70,70	up	0.3	27.22	81.6	79.63		
80,70,70	up	15.2	26.98	78.3			
80,70,70	up	24.9	26.98	79			
100,90,90	down	0.5	26.89	79.1	78.95	0.00	0.197
100,90,90	down						
100,90,90	down	13.5	26.89	78.8			
100,90,90	up	0.3	27.05	80.7	79.03		
100,90,90	up	15.6	26.96	78.5			
100,90,90	up	24.4	26.96	77.9			
90,90,100	down	0.5	26.91	79.8	79.65	-0.04	0.320
90,90,100	down						
90,90,100	down	13	26.91	79.5			
90,90,100	up	0.3	27.39	83.1	80.43		
90,90,100	up	15	27	79.1			
90,90,100	up	24.9	26.98	79.1			
70,80,70	down	0.5	26.96	80.5	80.50	0.03	0.383
70,80,70	down						
70,80,70	down	11	26.96	80.5			
70,80,70	up	0.2	27.59	83.5	79.83		
70,80,70	up	15	27.02	78.5			
70,80,70	up	23.9	26.98	77.5			
70,70,80	down	0.5	27	80.8	80.75	0.01	0.440
70,70,80	down						
70,70,80	down	10.1	27	80.7			
70,70,80	up	0.2	27.65	84.5	80.47		
70,70,80	up	15.3	27.04	78.7			
70,70,80	up	25.3	27.02	78.2			

Meldahl Lock and Dam
8/24/96

Dissolved Oxygen Data

Gate Setting	Location (up/down)	Sample Depth (feet)	Temperature (°C)	Percent Saturation	mean % saturation	Uncertainity % saturation
0.5	down	0.5	26.47	96.4	96.60	0.43
0.5	down	5	26.49	96.7		
0.5	down	12.5	26.49	96.7		
0.5	up	0.2	27.05	100.1	93.83	13.56
0.5	up	19.5	26.41	91.3		
0.5	up	34	26.38	90.1		
1	down	0.5	26.42	97.7	97.83	0.38
1	down	8.6	26.44	97.8		
1	down	16.7	26.44	98		
1	up	0.3	26.94	98.5	92.97	11.96
1	up	19.6	26.39	90.7		
1	up	34.8	26.35	89.7		
1.5	down	0.5	26.38	98.7	98.70	0.74
1.5	down	10.4	26.4	99		
1.5	down	20	26.4	98.4		
1.5	up	0.3	26.83	99.1	94.23	10.49
1.5	up	20.1	26.37	92.1		
1.5	up	36	26.35	91.5		
2	down	0.5	26.36	101.6	101.30	0.74
2	down	9	26.34	101.3		
2	down	18.6	26.34	101		
2	up	0.4	26.79	99.1	93.33	12.67
2	up	19.8	26.37	91.5		
2	up	34.8	26.33	89.4		
2.5	down	0.5	26.3	102.8	102.83	0.62
2.5	down	12.1	26.32	103.1		
2.5	down	22.5	26.23	102.6		
2.5	up	0.5	26.64	97.2	92.57	9.97
2.5	up	20.1	26.33	90.4		
2.5	up	36	26.3	90.1		
3	down	0.5	26.29	102.5	102.60	0.25
3	down	10.1	26.29	102.7		
3	down	17	26.29	102.6		
3	up	0.4	26.5	93.9	92.13	4.13
3	up	19.9	26.33	91.9		
3	up	34.5	26.31	90.6		
3.5	down	0.5	26.27	102.7	102.10	1.49
3.5	down	5	26.27	102.1		
3.5	down	10	26.27	101.5		
3.5	up	0.2	26.31	92.1	90.87	2.79
3.5	up	19.7	26.28	89.9		
3.5	up	35.6	26.28	90.6		
4	down	0.5	26.75	102.3	102.23	1.00
4	down	6	26.25	102.6		
4	down	10.6	26.25	101.8		
4	up	0.3	26.26	92.6	91.70	2.86
4	up	19.9	26.25	92.1		
4	up	34.3	26.28	90.4		
4.5	down	0.5	26.25	102.4	102.40	0.00
4.5	down	8.7	26.27	102.4		
4.5	down	16.3	26.25	102.4		
4.5	up	0.3	26.3	92.7	92.13	1.83
4.5	up	19.8	26.28	91.3		
4.5	up	33.9	26.3	92.4		
5	down	0.5	26.27	103.5	103.03	1.03
5	down	8.8	26.27	102.7		
5	down	19.8	26.29	102.9		
5	up	1.4	26.24	94.3	93.60	3.45
5	up	23.4	26.31	94.5		
5	up	36.3	26.33	92		

Belleville Lock and Dam
8/21/96

Dissolved Oxygen Data

Test Gate 1

Gate Setting	Location (up/down)	Sample Depth (feet)	Temperature (°C)	Percent Saturation	mean % saturation	Uncertainity % saturation
1	down	0.5	26.64	106.1	105.70	0.99
1	down	15.3	26.64	105.7		
1	down	25	26.64	105.3		
1	up	0.6	26.83	106.7	103.43	8.75
1	up	16.7	26.77	103.9		
1	up	29.1	26.65	99.7		
2	down	0.5	26.66	106.7	107.07	1.00
2	down	15.1	26.66	107.5		
2	down	23.7	26.66	107		
2	up	0.4	27.44	120.4	107.90	27.67
2	up	16.2	26.81	104.3		
2	up	29.5	26.65	99		
3	down	0.5	26.64	106	105.97	0.38
3	down	13	26.64	105.8		
3	down	18.4	26.64	106.1		
3	up	0.5	26.79	104.6	102.40	11.00
3	up	16.7	26.77	105.3		
3	up	29.4	26.54	97.3		
3.5	down	0.5	26.62	106.9	108.63	3.76
3.5	down	10	26.64	109.3		
3.5	down	17	26.62	109.7		
3.5	up	0.8	27.44	123.6	108.83	33.23
3.5	up	16.5	26.77	105.4		
3.5	up	29.6	26.56	97.5		
4	down	0.5	26.59	108.8	107.23	3.85
4	down	15.1	26.61	107.2		
4	down	24.4	26.57	105.7		
4	up	0.8	26.77	105.5	101.93	10.10
4	up	17.5	26.69	102.8		
4	up	29.4	26.5	97.5		

Montgomery Island Lock and Dam
8/19/96

Dissolved Oxygen Data

Gate Setting	Location (up/down)	Sample Depth (feet)	Temperature (°C)	Percent Saturation	mean % saturation	Uncertainity % saturation
0.5	down	0.5	24.66	105.1	105.27	1.90
0.5	down	5	24.66	106.1		
0.5	down	11	24.64	104.6		
0.5	up	0.8	26.1	122.3	109.93	26.65
0.5	up	13.4	24.24	104.5		
0.5	up	25	24.2	103		
1	down	0.5	24.75	106.8	106.77	0.38
1	down	10.1	24.77	106.9		
1	down	15	24.71	106.6		
1	up	1.3	26.4	119.4	108.77	22.88
1	up	13.2	24.24	103.8		
1	up	23.6	24.2	103.1		
1.5	down	0.5	24.71	108.9	108.63	1.15
1.5	down	10	24.73	108.1		
1.5	down	17.5	24.75	108.9		
1.5	up	0.5	26.21	120.4	108.63	25.52
1.5	up	12.7	24.31	104.1		
1.5	up	24.3	24.18	101.4		
2	down	0.5	24.75	109.9	109.07	2.11
2	down	10.2	24.9	108.2		
2	down	21	24.77	109.1		
2	up	0.6	25.6	117	106.60	22.37
2	up	12.2	24.26	101.1		
2	up	23.7	24.18	101.7		
2.5	down	0.5	24.71	110	109.70	0.66
2.5	down	14	24.62	109.5		
2.5	down	20	24.82	109.6		
2.5	up	0.4	25.73	116.1	107.77	17.98
2.5	up	12.2	24.33	104.2		
2.5	up	24	24.24	103		
3	down	0.5	24.8	109	108.90	0.66
3	down	10	24.82	109.1		
3	down	20	24.82	108.6		
3	up	0.5	26.01	118.2	106.77	24.84
3	up	12	24.35	102.5		
3	up	23.1	24.16	99.6		
3.5	down	0.5	24.62	108.4	108.73	0.76
3.5	down	9.2	24.71	109		
3.5	down	15.4	24.62	108.8		
3.5	up	0.5	25.5	117.5	107.47	21.60
3.5	up	12.3	24.38	102.9		
3.5	up	23.4	24.29	102		
4	down	0.5	24.58	107.3	107.70	0.99
4	down	5	24.51	107.7		
4	down	10	24.6	108.1		
4	up	0.5	25.58	115.4	107.53	17.56
4	up	12.7	24.55	105.5		
4	up	24.2	24.18	101.7		
4.5	down	0.5	24.49	107	106.60	1.14
4.5	down	6	24.47	106.7		
4.5	down	10	24.57	106.1		
4.5	up	0.7	25.01	107.9	103.67	10.19
4.5	up	14.3	24.44	103.4		
4.5	up	24.6	24.16	99.7		
spillway	down	0.5	24.41	107.2	106.77	0.94
spillway	down	5	24.4	106.5		
spillway	down	9.3	24.42	106.6		
spillway	up	0.1	24.49	101.8	101.60	4.74
spillway	up	17	24.51	103.4		
spillway	up	33.5	24.2	99.6		

Smithland Lock and Dam
8/29/96

Dissolved Oxygen Data

Gate Setting	Location (up/down)	Sample Depth (feet)	Temperature (°C)	Percent Saturation	mean % saturation	Uncertainity % saturation
0.5	down	0.5	28.46	85	84.70	1.08
0.5	down	12.3	28.46	84.9		
0.5	down	21.2	28.46	84.2		
0.5	up	0.2	28.62	82	82.20	0.43
0.5	up	15.5	28.58	82.3		
0.5	up	29.8	28.58	82.3		
1	down	0.5	28.56	84.3	84.17	0.57
1	down	14	28.56	84.3		
1	down	20.5	28.56	83.9		
1	up	0.3	28.7	81.8	81.00	1.72
1	up	15.4	28.68	80.6		
1	up	30.2	28.68	80.6		
1.5	down	0.5	28.62	85.4	85.50	0.25
1.5	down	15.5	28.64	85.5		
1.5	down	28	28.64	85.6		
1.5	up	0.4	28.72	82.1	81.30	1.74
1.5	up	15.3	28.68	80.8		
1.5	up	31.6	28.7	81		
2	down	0.5	28.89	90.2	89.83	1.37
2	down	10	28.91	90.1		
2	down	16	28.85	89.2		
2	up	0.3	28.94	93.8	87.03	14.55
2	up	15.3	28.84	83.7		
2	up	28.8	28.82	83.6		
2.5	down	0.5	28.85	89.4	89.50	1.27
2.5	down					
2.5	down	7.2	28.87	89.6		
2.5	up	0.3	28.77	88.8	88.63	2.88
2.5	up	15	28.79	89.7		
2.5	up	31.6	28.73	87.4		
3	down	0.5	28.83	91.1	90.73	1.00
3	down	7	28.85	90.8		
3	down	13	28.83	90.3		
3	up	0.4	29.07	95.6	83.27	37.18
3	up	15.2	28.75	87.6		
3	up	29.6	28.77	66.6		
3.5	down	0.5	28.85	92.4	92.00	1.31
3.5	down	7.7	28.85	92.2		
3.5	down	14	28.85	91.4		
3.5	up	0.2	29.01	96.2	91.67	9.90
3.5	up	15.2	28.83	88.7		
3.5	up	31.1	28.83	90.1		
4	down	0.5	28.95	94.5	94.13	0.87
4	down	6	28.95	94.1		
4	down	13	28.95	93.8		
4	up	0.4	29.05	91.3	90.47	2.11
4	up	15.2	29.03	90.5		
4	up	29.1	29.01	89.6		
4.5	down	0.5	28.95	94.8	94.63	0.52
4.5	down	7	28.93	94.7		
4.5	down	15	28.95	94.4		
4.5	up	0.4	29.12	92.5	95.70	8.34
4.5	up	15.3	29.11	95.4		
4.5	up	29.5	29.05	99.2		
5	down	0.5	28.91	95.4	95.33	0.29
5	down	7.2	28.91	95.2		
5	down	10.5	28.97	95.4		
5	up	0.5	29.09	93.4	92.77	2.31
5	up	15.1	29.2	93.2		
5	up	27	29.14	91.7		

Racine Hydropower
9/15/95

	Sat Temp (C)	Temp based Sat Conc
Dissolved Oxygen Data	25.55	8

Gate Setting %	Discharge	time	Location (up/down)	Sample Depth (feet)	Concentration mg/l	mean concentration	Efficiency	Uncertainity in Efficiency
91		14.29	down	surface	5.65	5.63	0.11	0.124
91			down	middle	5.6			
91			down	bottom				
91		14.26	up	surface	5.36	5.32		
91			up	middle	5.27			
91			up	bottom	5.32			
70		13.58	down	surface	5.54	5.52	0.09	0.105
70			down	middle	5.5			
70			down	bottom				
70		13.55	up	surface	5.25	5.27		
70			up	middle	5.23			
70			up	bottom	5.34			
55		13.1	down	surface	5.54	5.52	0.07	0.100
55			down	middle	5.49			
55			down	bottom				
55		13.07	up	surface	5.45	5.32		
55			up	middle	5.25			
55			up	bottom	5.27			
45		11.51	down	surface	5.42	5.34	-0.04	0.595
45			down	middle	5.25			
45			down	bottom				
45		11.53	up	surface	5.92	5.44		
45			up	middle	5.24			
45			up	bottom	5.17			
35		11.27	down	surface	5.66	5.67	0.15	0.042
35			down	middle	5.67			
35			down	bottom				
35		11.22	up	surface	5.31	5.27		
35			up	middle	5.27			
35			up	bottom	5.22			